MONITORING AGENCY DOCUMENT NO: ARL 240
ASTIA DOCUMENT NO: AD
GRANT AF-EOAR-61-42. TN NO. 3

SI Publ. No. 338

273 214

NOX
62-2-5

CATALOGED BY ASTIA
AS AD No. 273214

TECHNICAL NOTE

OXIDATION OF TANTALUM AT 300-550° C

Per Kofstad

CENTRAL INSTITUTE FOR INDUSTRIAL RESEARCH
BLINDERN - OSLO - NORWAY

NOVEMBER 1961

ASTIA
RECEIVED
MAR 23 1962
TISIA

This research was supported in whole, or in part by the Metallurgy and Ceramics Branch, ARL, Office of Aerospace Research, United States Air Force, monitored by the European, Office, Office of Aerospace Research under Grant No. AF-EOAR-61-42.

MONITORING AGENCY DOCUMENT NO:
ASTIA DOCUMENT NO: AD
GRANT AF-EOAR-61-42. TN NO. 3

SI Publ. No. 338

TECHNICAL NOTE

OXIDATION OF TANTALUM AT 300-550° C

Per Kofstad

CENTRAL INSTITUTE FOR INDUSTRIAL RESEARCH
BLINDERN - OSLO - NORWAY

NOVEMBER 1961

This research was supported in whole, or in part by the Metallurgy and Ceramics Branch, ARL, Office of Aerospace Research, United States Air Force, monitored by the European, Office, Office of Aerospace Research under Grant No. AF-EOAR-61-42.

ABSTRACT

The oxidation behaviour of tantalum at 300° to 550 °C has been studied. The work comprises gravimetric oxidation rate measurements and x-ray diffraction, electron diffraction, electron microscopy, metallographic and microindentation hardness studies of oxidized specimen. Direct x-ray diffraction and metallographic observations have also been made on specimens during oxidation.

The oxidation constitutes oxygen dissolution in the metal, formation of the metallic oxide phases TaO_y and TaO_z, and formation of Ta_2O_5. The relative importance of the various part-processes involved in the oxidation is a function of temperature, oxygen pressure, and time of oxidation.

Initial oxidation below 450 °C conforms with a logarithmic oxidation. This is interpreted in terms of a rate-determining nucleation and formation of the metallic oxide phases. Over longer periods and during initial oxidation at higher temperatures the oxidation is approximated by a parabolic oxidation behaviour which mainly constitutes a rate-determining oxygen dissolution in the metal and associated metallic oxide formation. Above 450 °C the initial approximate parabolic oxidation is followed by a breakaway oxidation which is associated with Ta_2O_5-formation. The breakaway oxidation is interpreted in terms of an oxygen chemisorption equilibrium followed by a rate-determining reaction governed by nucleation and growth of Ta_2O_5-nuclei[1].

CONTENTS

OXIDATION OF TANTALUM IN THE TEMPERATURE RANGE 300-550 °C.

1.0 INTRODUCTION

Tantalum has in recent years received considerable attention as a possible high temperature material. Tantalum has a melting point close to 3000 °C and it also has excellent ductility which makes it one of the most workable refractory metals. A major shortcoming of tantalum as a high temperature material is its great reactivity with oxygen and other gases at elevated temperatures, and in considering application of tantalum detailed knowledge of the oxidation behaviour is required.

The present work constitutes part of an extended study of the oxidation behaviour of tantalum1). The present paper deals with oxidation of tantalum in oxygen at 300° to 550 °C. The experimental work includes oxidation rate studies by means of gravimetric techniques and investigations on oxidized specimens by means of X-ray and electron diffraction, electron microscopy, and metallographic techniques.

2.0 LITERATURE

2.1 Tantalum-Oxygen System

2.11 Tantalum-oxygen solid solutions. Oxygen is dissolved interstitially in the b.c.c. lattice of tantalum$^{2-12)}$. According to Gebhardt and Seghezzi$^{2,3)}$ the solubility increases from 1.5 to 6.4 at% from 700° to 1650 °C. The same authors$^{2)}$ observed that oxygen dissolution causes a linear increase in the lattice parameter from 3.3025 Å for the pure metal to 3.316 Å at 3.6 at% O. This is shown in Fig. 1.

Diffusion of oxygen in tantalum has been studied by internal friction and microindentation hardness measurements$^{6-12}$. Powers and Doyle^{11} give a mean value of the diffusion coefficient of $D = 0.0044 \exp(-\frac{25450}{RT})$ at low oxygen concentrations (<0.15 at%). At higher oxygen concentrations, effects due to interaction and association of interstitial oxygen atoms were observed. At a concentration of 1.07 at% oxygen the value of the diffusion coefficient was found to be approximately $D = 0.01 \exp(-\frac{27700}{RT})^{9,10}$.

2.12 Tantalum oxides. The formation of metallic oxide phases (or suboxides) of tantalum has been the subject of several investigations. The orthorhombic phase termed TaO_y has been found as an oxidation product in low temperature oxidation (300° to 500 °C) of tantalum$^{13,16,17)}$. Schönberg^{5} found the unit cell dimensions of TaO_y to vary between a = 7.194 Å, b = 3.266 Å, c = 3.204 Å, and a = 7.238 Å, b = 3.273 Å, c = 3.216 Å. The same author suggested TaO_y to have the composition Ta_4O. Attempts to prepare Ta_4O by argon arc melting of stoichiometric mixtures of Ta and Ta_2O_5 have proved unsuccessful$^{17)}$.

Another metallic oxide phase termed TaO_z has been observed in several studies of oxidation of tantalum[13-17]. According to Norman[16] TaO_z has a tetragonal structure with unit cell dimensions of $a = 6.68_0$ Å, $b = 4.75_8$ Å. Electron probe x-ray microanalysis suggest a wide homogeneity range for this oxide with an approximate composition of TaO_2[16]. TaO_z is observed as oxide platelets extending into the metal from the metal surface[15,17]. Pawel and Cathcart[15] have established that the oxide platelets grow parallell to the $\{320\}$ sets of planes of the metal. Attempts to synthesize TaO_z by argon arc melting of mixtures of Ta and Ta_2O_5 have not been successful[17].

Oxides with probable compositions TaO and TaO_2 were reported by Schönberg[5]. TaO is of the sodium chloride structure, while TaO_2 is isomorphous with rutile. The existence of TaO and TaO_2 has, however, been questioned by both Wasilewski[4] and Lagergren and Magnéli[18].

An intermediate oxide in the TaO_2 - Ta_2O_5 interval was reported by Schönberg[5]. The structure was complicated and was neither related to TaO_2 nor to that of Ta_2O_5.

Ta_2O_5 has been found to exist in two modifications with a transition temperature of 1320 ± 20[4,18]. The low temperature phase β-Ta_2O_5 is isomorphous with the low-temperature modification of Nb_2O_5. Schäfer[13] suggests that Ta_2O_5 is the only thermodynamically stable oxide of tantalum.

2.2 Oxidation of Tantalum.

Various aspects of oxidation of tantalum has been studied[1,3,19-32]. At 50° to 300 °C Vermilyea[23)] found the kinetics consistent with the Mott-Cabrera theory. Above 300 °C oxygen dissolution in the metal was appreciable. Gulbransen and Andrew[19,20)] interpreted the oxidation of tantalum at 250° to 450 °C in terms of a parabolic behaviour with an activation energy of 27.4 kcal/mole. Waber et al.[27] found the oxidation in air to be logarithmic at 220° to 320 °C, while no unambiguous distinction could be made between logarithmic or parabolic oxidation at 320° to 350 °C. Assuming parabolic oxidation the activation energy was found to be 27.2 kcal/mole. Waber[28)] later replotted the data and found them in agreement with a cubic oxidation.

Cathcart et al.[29,30] studied oxidation of tantalum at 400° to 530 °C. The oxidation was interpreted in terms of an initial protective stage. A subsequent increase in the oxidation rate was suggested to be a result of cracks and blisterlike ruptures in the oxide (Ta_2O_5).

Peterson et al.[21)] studied the temperature and oxygen pressure dependence at 500° to 1000 °C and at oxygen pressures of 1/2 to 40.8 atm. Similar studies at 600° to 800 °C and in the oxygen pressure range 1-760 torr were carried out by Cowgill and Stringer[26)]. In both cases the oxidation was interpreted in terms of an equilibrium adsorption process prior to the rate-determining step of the linear oxidation.

The oxidation behaviour of tantalum at 500° to 700 °C and at oxygen pressures 760 to 0.1 torr was studied by Kofstad[1)]. The initial oxidation was found to constitute oxygen dissolution in the metal and the formation of the metallic oxide phases TaO_y and TaO_z. A subsequent transition to a linear breakaway oxidation was found to be associated with Ta_2O_5- formation. The linear oxidation was interpreted in terms of an oxygen chemisorption equilibrium followed by a rate-determining reaction governed by nucleation and growth of Ta_2O_5- nuclei.

Albrecht et al.[32)] found the oxidation in 1 atm. oxygen to be linear at 500° to 1250 °C. At 1000 °C the reaction followed a square root of pressure dependence. In addition to oxide scale formation, oxygen was found to diffuse into the base metal during oxidation, The simultaneous oxygen dissolution and oxide formation at 700° to 1420 °C and at oxygen pressures of 1 x 10^{-3} to 2 x 10^{-2} torr was studied by Seghezzi[3)].

3.0 MATERIALS AND METHODS

3.1 Materials

Electron beam melted tantalum obtained from the Stauffer-Temescal Company, U.S.A., was used in the studies. The metal was received in the form of 1.5 mm thick plates. Estimates of impurities are given in Table I.

The tantalum metal was cold-rolled to a thickness of 0.1 to 0.3 mm and cut into specimens with dimensions 1.5 by 2 cms. Prior to oxidation the specimenswere polished with alumina, rinsed in distilled water and acetone, and subsequently chemically polished for 10 sec. in a solution consisting of 10 parts H_2SO_4, 4 parts 70 % HNO_3, and 3 parts HF. To study the effect of pretreatement of the metal, specimens were also in cases annealed for 1/2 hr. in high vacuum ($< 10^{-5}$ torr) at 1400 °C.

The oxygen employed was commercial tank oxygen (99.8 % purity) which was dried over phosphorus pentoxide.

3.2 Methods

The rate of oxidation of tantalum was measured gravimetrically by means of microtorsion balances. The weight gain could be read to better than ± 0.5 $\mu g/cm^2$. Prior to start of oxidation the oxidation apparatus was evacuated to a pressure 10^{-5} torr. Detailed descriptions of both the apparatus and the procedure employed has been given elsewhere[1,33,34].

X-ray diffraction investigations were carried out by means of a General Electric XRD-3 recording X-ray diffractometer.

TABLE I

Analysis of high-purity, electron beam-melted tantalum obtained from the Stauffer-Temescal Company

Impurity	Amount present w/o
Carbon	0.006
Nitrogen	<0.002
Tungsten	0.10
Aluminium	<0.002
Cobalt	<0.002
Chromium	<0.002
Copper	<0.004
Iron	<0.005
Magnesium	<0.002
Manganese	<0.002
Nickel	<0.002
Lead	<0.002
Silicon	<0.01
Titanium	<0.005
Vanadium	<0.002
Molybdenum	0.008
Tin	<0.004
Niobium	0.05
Oxygen	0.006

The metallographic and microhardness indentation testing were performed with a Reichert universal camera microscope (Model MeF) and a Reichert microhardness tester (No. 1109) using a Vickers pyramid. The specimens for metallographic studies were mounted in Araldit Giess Harz D. As etchant in the metallographic studies was used a solution consisting of 170 ml nitric acid (sp. gr. 1.4), 50 ml hydrofluoric acid (sp. gr. 1.16), 510 ml methanol, and 5 g citric acid[35].

The electron microscope studies were made with an RCA EMU 2D electron microscope. The procedure for preparing specimens for such studies has been given elsewhere1,33).

4.0 EXPERIMENTAL RESULTS

4.1 Oxidation rate measurements.

The results of the oxidation rate measurements on cold-rolled, unannealed tantalum in 1 atm. oxygen in the temperature range 300°- 550 °C are shown in Figs. 2-5. The oxidation curves represent averages of 4 or more runs. In Figs. 2-4 the weight gain has been plotted as a function of time, and the experimental results are represented by the fully drawn curves. Mostly the oxidation were followed for 300 min. as shown in Fig. 2 and 4. In a few cases the oxidation was followed for periods up to 3 days. This is shown in Fig. 3.

At temperatures above 450 °C one observes - within the time periods studied - a transition to a faster breakaway oxidation (Fig. 4). The time period until this change in kinetics occurs, becomes shorter with increasing temperature. At 475 °C the corresponding transition takes place after approximately 600-700 min.

The results were generally only reproducible to ± 15 %. Despite careful preparations of the samples it was also difficult to obtain satisfactory reproducibility as to the duration of the incubation period for the breakaway oxidation. In this respect the results may be estimated to be reproducible to within 40 %. The rate of breakaway oxidation, however, was reproducible to within ± 10 %.

In many cases it is difficult to describe the oxidation behaviour of tantalum over longer periods of time in terms of definite rate equations. The results of the initial oxidation at the lower temperatures suggest some type of logarithmic oxidation behaviour. This is shown in Fig. 5a, where the weight gain is plotted as a function of logarithm of time.

As seen in Fig. 5a the oxidation over longer periods of time proceeds faster than that of the logarithmic oxidation. Under these conditions the oxidation is approximated by a parabolic oxidation. This behaviour is also suggested for the initial oxidation at temperatures above 450 °C. The parabolic behaviour is indicated in Fig. 3 where the stippled lines represents parabolic oxidation and in Fig. 5b where weight gain has been plotted as a function of square root of time.

The breakaway oxidation is initially sigmoidal. After this initial period of the breakaway oxidation one observes a slight decrease in the oxidation rate which eventually becomes approximately constant (linear oxidation).

The effect of oxygen pressure on the rate of oxidation at 400° and 450 °C is shown in Figs. 6 and 7. In some cases rather rapid changes in the kinetics were also observed resulting in rather uneven oxidation with time. The general conclusion which may be drawn from these measurements is that the initial oxidation is oxygen pressure dependent, while during later stages the rate of oxidation becomes approximately independent of oxygen pressure. It is difficult to establish the rate equation for the initial oxidation at the lower oxygen pressures. This in turn makes it difficult to evaluate the corresponding oxygen pressure dependence.

Studies of oxidation of specimens annealed in high-vacuum for 1/2 hr. at 1400 °C were carried out in 1 atm. oxygen. Within the limits of error no difference in oxidation behaviour was observed compared to that of unannealed specimens. However, the results suggest on an average oxidation rate about 10 % higher for the annealed specimens. Also the time period before the transition to a breakaway oxidation was generally longer for these than for the corresponding unannealed specimens.

In a few cases tantalum-oxygen alloys containing 2 at% O were prepared by oxidation at 400° - 450 °C in 1 atm. oxygen with subsequent anneal for 2 hrs. in high-vacuum at 900 °C. The alloy composition were determined from the weight gain of the specimens. Subsequent oxidation showed a somewhat slower rate of oxidation for these alloys. The results at 450 °C and 1 atm. oxygen is shown in Fig. 7. Within the limits of error there was at 500 °C no difference in the time period before the transition to breakaway oxidation compared to unalloyed tantalum.

4.2 X-ray diffraction studies of oxidized specimens.

A number of specimens oxidized under different conditions of temperature and oxygen pressure were studied by X-ray diffraction. In a few cases X-ray diffraction studies were also carried out directly on specimens undergoing oxidation. This was done by employing a specially constructed furnace in connection with the X-ray diffraction unit.

A characteristic feature of the oxidation behaviour of tantalum in the temperature range 300° - 500 °C is the great importance of oxygen dissolution in the metal as evidenced by an increase in the lattice parameter of the metal in the outer layer of the metal. This was also confirmed by microindentation hardness measurements (see later section). To study oxygen dissolution, lattice parameter determinations were made directly on the oxidized surface. In Table II are shown values observed after oxidation in 1 atm. oxygen for various lengths of time at temperatures 350° to 475 °C. The values of the lattice parameters were determined from the (004) reflection employing Ni-filtered Cu-radiation.

TABLE II

Values of the lattice parameter of tantalum as determined by measurements directly on the oxidized surface. Oxidation at 1 atm. oxygen.

Oxidation temperature	Time of oxidation	Lattice parameter
350 °C	1700 min	3.318 Å
350 °C	4600 min	3.320 Å
400 °C	3160 min	3.328 Å
400 °C	4600 min	3.328 Å
450 °C	1660 min	3.320 Å
450 °C	3120 min	3.308 Å
475 °C	300 min	3.320 Å

The parameter as determined on the surface of unoxidized tantalum was found to be 3.304 Å. As seen from Table II an appreciable increase in the parameter takes place during oxidation. By comparing with the results of Gebhardt and Seghezzi on the variation in lattice parameter with oxygen content (Fig. 1), it is seen that values of 3.320 and 3.328 Å corresponds to oxygen concentrations of 4-5 and 6-7 at%, respectively in the outer layers of the metal.

A second characteristic feature of the results is that the oxidation leads to the formation of the metallic oxide phases TaO_y and TaO_z. TaO_y is primarily formed at the lower temperatures ($< \sim 450$ °C) and during initial periods of oxidation, while TaO_z is primarily formed at higher temperatures and after longer periods of oxidation.

Below 450 °C and within the time periods studied (up to 4600 min) no Ta_2O_5-formation could be detected neither by x-ray nor by electron diffraction. At temperatures above 450 °C Ta_2O_5 could not be detected by x-ray diffraction during initial periods which correspond approximately to the observed incubation period for the breakaway oxidation in the oxidation rate measurements. The breakaway oxidation, on the other hand, was found to be associated with heavy Ta_2O_5-formation. X-ray diffractograms of specimens during the initial formation of Ta_2O_5 showed sharp diffraction lines indicating well developed crystallinity of the initial traces of Ta_2O_5.

X-ray diffraction studies of the oxidation products were also carried out directly on specimens undergoing oxidation by employing a furnace in connection with the x-ray diffraction unit. These studies were in agreement with the abovementioned results. The metallic oxide phases TaO_y and TaO_x are thus formed at temperature during oxidation and are not a result of a precipitation during cooling of the specimen to room temperature.

A summary of the x-ray diffraction studies is given in Table III. From these results the approximate limits for the first detection of TaO_z and Ta_2O_5 by x-ray diffraction may be estimated. This is shown graphically in Fig. 8 in which oxidation temperatures has been plotted as a function of time of oxidation. The metallic oxide phases are of course present in amounts undetectable by x-ray diffraction at oxidation periods shorter than that indicated in Fig. 8. This was particularly evident in comparitive x-ray diffraction and metallographic studies on the same specimens. In such studies it was shown that TaO_z often could be detected earlier and more easily by metallographic observations than by x-ray diffraction.

TABLE III

Summary of X-ray diffraction studies on specimens oxidized in the temperature range, 300° to 550 °C

Oxidation temperature	Oxygen pressure	Time of Oxidation	Phases observed	
200 °C	1 atm	300 min	Ta	(Ta-powder)
300 °C	1 atm	240 min	Ta, TaO_y	(Ta-powder)
350 °C	1 atm	300 min	Ta, TaO_y	
350 °C	1 atm	1680 min	Ta, TaO_y	
350 °C	1 atm	4620 min	Ta, TaO_y	
400 °C	1 atm	300 min	Ta, TaO_y	
400 °C	1 atm	1390 min	Ta, TaO_y	
400 °C	1 atm	4600 min	Ta, TaO_y, TaO_z	
400 °C	10 torr	300 min	Ta, TaO_y	
400 °C	10 torr	1740 min	Ta, TaO_y, traces of TaO_z	
400 °C	0.1 torr	300 min		
450 °C	1 atm	300 min	Ta, TaO_y, possible traces of TaO_z	
450 °C	1 atm	300 min	Ta, TaO_y	
450 °C	1 atm	1660 min	Ta, TaO_y, TaO_z	
450 °C	1 atm	1710 min	Ta, TaO_y, TaO_z. traces of Ta_2O_5	
450 °C	1 atm	3120 min	Ta, TaO_y, TaO_z, traces of Ta_2O_5	
450 °C	10 torr	300 min	Ta, TaO_y, TaO_z	
450 °C	10 torr	300 min	Ta, TaO_y, TaO_z	
450 °C	0.1 torr	300 min	Ta, TaO_y	
475 °C	1 atm	300 min	Ta, TaO_y, TaO_z	
475 °C	1 atm	1740 min	Ta, TaO_z, Ta_2O_5	
500 °C	1 atm	10 min	Ta	
500 °C	1 atm	60 min	Ta, TaO_z	
500 °C	1 atm	300 min	Ta, TaO_z, Ta_2O_5	
500 °C	10 torr	300 min	Ta, TaO_y, TaO_z, traces of Ta_2O_5	
500 °C	10 torr	300 min	Ta, TaO_z traces of Ta_2O_5	
500 °C	10 torr	300 min	Ta, TaO_y, TaO_z (specimen annealed before oxidation)	
500 °C	10 torr	400 min	Ta, TaO_y, TaO_z, traces of Ta_2O_5	
500 °C	0.1 torr	300 min	Ta	
500 °C	0.1 torr	1740 min	TaO_z, Ta_2O_5	
550 °C	1 atm	10 min	Ta, TaO_z	
550 °C	1 atm	60 min	Ta_2O_5, TaO_z beneath Ta_2O_5-layer	
550 °C	0.1 torr	300 min	TaO_z, Ta_2O_5	

The x-ray diffraction studies suggest that oxidation in the indicated temperature region involves the following sequence of steps:

$$\mathrm{Ta} \longrightarrow \begin{matrix}\text{Ta-O solid sol'n}\\ \mathrm{TaO}_y\end{matrix} \longrightarrow \mathrm{TaO}_z \longrightarrow \mathrm{Ta}_2\mathrm{O}_5 \tag{1}$$

4.3 Surface appearances of oxidized specimens.

During very initial stages of oxidation visual examination of the specimens showed no evidence of oxide film formation. After increased oxidation the specimens took on apparent interference colours. However, these did not show the normal sequence of interference colours; rather these tended in almost all cases towards blue or violet-blue. The interference colours were observed under conditions where x-ray diffraction studies show formation of relatively large amounts of the metallic oxide phases TaO_y and TaO_z.

During the transition period to the breakaway oxidation the specimens became grey or spotty grey. After prolonged oxidation in the linear oxidation region at temperatures above 500 °C the surface oxide-consisting of Ta_2O_5-turned grey-white and white.

4.31 Metallographic studies. A characteristic feature of specimens oxidized under conditions where only the metallic oxide phases - particlularly TaO_z - could be detected by x-ray diffraction, is the appearance of regular patterns of oxide platelets which extend from the metal surface into the metal. The oxide platelets could best be examined by observation directly on the oxidized surface and after polishing and etching of the surface. Numerous studies were carried out in this respect. In the following a few examples are given of both the formatiin of oxide platelets and the initial formation of Ta_2O_5. Detailed accounts of both the x-ray diffraction and metallographic studies of the oxide platelets have been given elsewhere[16,17]. These latter studies have shown that the oxide platelets consist of the metallic oxide phase TaO_z. The same studies furthermore indicate that the TaO_y phase can not be distinguished metallographically from the metal phase.

Fig. 9 shows the surface of a cold-rolled (from 1.5 to 0.1 mm thickness), unannealed Ta-specimen after oxidation for 3200 min at 350 °C and 1 atm. O_2. The specimen was polished and etched before oxidation. No distinct grain boundaries are observed, and correspondingly the oxide platelets are seen to form in more or less regular pattern only within small areas of the surface.

In high-vacuum annealed specimens the oxide platelets are formed in regular patterns within the individual grains of the metal. This is shown in Figs. 10 a and b, which refer to a specimen oxidized for 3200 min at 400 °C and 1 atm. O_2. The regular patterns of the oxide platelets is due to the fact that they grow parallell to the $\{320\}$ planes of the metal[15,17]. In Fig. 10 b it is also seen that grain boundaries in cases appear to favor the formation of the oxide platelets, e.g. that grain boundaries serve as relative effective nucleation sites for the oxide platelet formation. The number of platelets are also seen to vary considerably from grain to grain.

The oxide platelets extend down into the metal and their depth of penetration is a function of length of oxidation. After polishing and etching of the oxidized surface the platelets are still observed as shown in Fig. 11, which refers to the same area as shown in Fig. 10b, but at a higher magnification. Such studies also showed that the density of platelets decreased with increasing distance from the metal surface. This is concluded to be due to difference in size of the individual platelets.

Figs. 12 a-d show sections of the surface of the same specimen oxidized for 300 min at 500 °C and 10 torr O_2. The specimen was high-vacuum annealed, polished and etched before oxidation. The oxidation of this specimen was stopped during the transition to the breakaway oxidation. As seen, an uneven oxidation of the surface takes place. The oxidation constitutes platelet formation. The dark, somewhat diffuse parts of the oxide are believed to represent the initial formation of Ta_2O_5. This takes place at or on top of oxide platelets in the metal. Fig. 12d shows a polishing streak in the metal and this appears to favor the formation and crystallization of oxide phases. This is concluded to be due to the presence of strain energies in this part of the metal.

After polishing off the outer layer of the specimen, it appeared completely metallic. Etching, however, brought forth the regular pattern characteristic of the suboxide platelets. This is shown in Fig. 13, which refers to the same specimens as shown in Fig. 12. At a higher magnification the grey-black etch-lines were found to have lamellar appearance and to consist of closely-spaced oxide platelets. This is seen in Fig. 14.

By oxidizing a correspondingly annealed tantalum specimen for 400 min but otherwise under identical conditions (500 °C and 10 torr oxygen) very distinct formation of Ta_2O_5 are observed on the surface. After polishing and etching of the oxidized surface the characteristic pattern of suboxide platelets are again observed as shown in Fig. 15. In Fig. 15 are also seen remnants of unremoved Ta_2O_5 on the same specimen.

A section of a correspondingly polished and etched specimen after oxidation for 1300 min at 600 °C and 10^{-2} torr also shows the formation of Ta_2O_5 on top of TaO_z platelets. In this case TaO_z are also present as flakes or platelets parallell to the surface. Ta_2O_5 is only formed on top of TaO_z and is represented by the darker grey parts on the TaO_z-flakes.

Direct metallographic observations of the oxidation at temperature were also made by means of hot-stage microscopy36). In such studies the formation of the oxide platelets may be followed directly and the results are in agreement with the results described above. During breakaway oxidation involving heavy Ta_2O_5-formation, the oxide is seen to crack. In cases these cracks takes the form of blisterlike or "volcanic" ruptures. These are believed to be a result of a more rapid Ta_2O_5-formation in local areas on the metal surface which forces and breaks up surface the oxide above.

4.32 Electron microscopy studies. The surface of oxidized specimens were also studied by electron microscopy. In general these studies give the same information as the corresponding metallographic observations. The experimental results are in good agreement with similar electron microscope studies by Cathcart et al.[29,31]. At the lowest temperatures the characteristic formation of oxide platelets are observed. Examples of these are shown in Fig. 17 and 18 which refer to unannealed tantalum specimens oxidized at 350° and 450 °C, respectively. As in the metallographic studies an uneven attack of the metal was observed.

Non-uniform oxidation became particularly marked during the transition to the breakaway oxidation. Under these conditions some areas would predominantly show oxide platelets, while other areas appeared to be covered by a more pronounced scale, often with blisterlike ruptures. Examples of such surfaces are given in Figs. 19 a,b, and c which refer to specimen oxidized for 300 min at 500 °C and 10 torr oxygen. The more pronounced oxide scale with ruptures are suggested to reflect the formation of Ta_2O_5, which initially takes place in spots and local areas on the surface.

4.33 Microindentation hardness measurements. The hardness of tantalum increases with increasing oxygen content in the metal. In order to obtain a measure of the importance of oxygen dissolution in the metal microindentation measurements were thus carried out on oxidized specimens. Results of such measurements are shown in Figs. 20-22, in which microhardness has been plotted as a function of distance from the metal surface. Oxygen penetration from two opposite surfaces as measured by microindentation hardness measurements were seldom found to be exactly symmetrical.

The results in Fig. 20 refer to a unannealed Ta specimen oxidized for 1680 min at 350 °C and 1 atm. oxygen. As seen an appreciable oxygen diffusion into the metal takes place even at 350 °C. This is of course expected considering the rapid rate of oxygen diffusion in tantalum. Assuming the diffusion coefficient of oxygen in tantalum to be $D = 0.01 \exp\left(-\frac{27700}{RT}\right)$, the mean square displacement $\Delta\bar{x} = \sqrt{2Dt}$, is after oxidation for 1680 min at 350 °C calculated to be $\Delta\bar{x} = 6.1\mu$. This is in satisfactory agreement with the experimental results when considering the approximate nature of the microindentation hardness measurements.

Corresponding measurements on unannealed Ta specimens oxidized at 400 °C and 1 atm. oxygen for 300 and 1740 min, respectively, are shown in Fig. 21. Oxygen penetration increases with increasing length of oxidation. The specimens had thicknesses of 93 and 86μ, respectively, and after 1740 min it appears that appreciable amounts of oxygen have penetrated to the middle of the specimen. The decrease in microhardness at the surface is believed to result from the presence of metallic oxide phases in the outer layer of the metal.

Microhardness indeatation measurements were made on unannealed and annealed specimens oxidized under identical conditions. The annealing caused a reduction in the hardness of the specimen, and in Fig. 22 are shown the increase in microhardness above the original value as a function of distance from the metal surface. The specimens were oxidized for 300 min at 500 °C and 10 torr oxygen. The results suggest a somewhat larger depth of penetration in the annealed specimen.

5.0 DISCUSSION

Tantalum has a complex oxidation behaviour. In the temperature range 300° - 550 °C, oxidation in pure oxygen involves oxygen dissolution in the metal, formation of the two metallic oxide phases of tantalum TaO_y and TaO_z, and formation of Ta_2O_5. The relative importance of the various part-processes is a function of temperature, oxygen pressure, and time of oxidation. Thus, Ta_2O_5 has not been detected on oxidized specimens at temperatures below 450 °C within the time periods (up to 4600 min.) employed in the present studies.

Under many conditions in the indicated temperature range the oxidation behaviour over longer periods of time may not be described in terms of definite rate equations. The initial oxidation at the lowest temperatures may be approximated by a logarithmic oxidation behaviour. Over longer periods of time the oxidation proceeds faster than that of a logarithmic oxidation, and under these conditions the oxidation behaviour may be described by an approximate parabolic rate equation. This latter relationship also gives an approximate description of the initial oxidation at the higher temperatures. The breakaway oxidation is initially sigmoidal; however, over longer periods of time the rate of the breakaway oxidation becomes approximately constant (linear oxidation).

5.1 Oxygen dissolution in the metal. The experimental results show that oxygen dissolution in the metal is of primary importance. The x-ray diffraction studies show that the oxygen concentration in the outer layer of the metal rapidly reaches concentrations of 5 to 7 at%. The microindentation hardness measurements show penetration distances for oxygen in tantalum which is in satisfactory agreement with calculated values. The latter values have been estimated on the basis of the diffusion coefficient for oxygen in tantalum as determined by internal friction studies[9,10]. The oxygen penetration into the metal also apparently to some extent depends upon the pretreatment of the metal, as the oxygen has been found to penetrate further into the metal for annealed than for unannealed specimens (Fig. 24).

The equilibrium solubilities of oxygen in tantalum at high temperatures have been found to varv from 1.5 to 6.4 at% from 700° to 1650 °C[2,3]. Extrapolation of these data suggest an equilibrium solubility of 0.7 to 0.8 at% at 400° to 450 °C. The measured oxygen concentrations in the outer layers of the metal thus indicate a very large supersaturation of oxygen. However, the measured solubilities at high temperatures[2,3] apparently reflect equilibria of tantalum-oxygen solid solutions with Ta_2O_5. In the present oxidation studies the large oxygen concentrations in the outer layer of the metal have been found under conditions where no Ta_2O_5 has been observed on the oxidized specimens. Thus the observed oxygen concentrations probably reflect the approximate solubility of oxygen in tantalum in quasi-equilibrium with the metallic oxide phases. As a further confirmation of these considerations it is found that the oxygen concentration in the outer layers of the metal decreases when the first traces of Ta_2O_5 is formed on the surface (see Table II, 450 °C, 3120 min.)[1]. It is also important to note that due to the large stresses and strains involved in the nucleation of oxide phases some degree of supersaturation of oxygen in tantalum is necessary before the formation of the metallic oxide phases takes place[15].

By combining the diffusion data ($D = 0.01 \exp -\left(\frac{27700}{RT}\right)$ 9,10) and the value of the oxygen content at the metal surface, estimates may be made of the expected weight gain due to oxygen dissolution alone37). Taking a value of 5 at% for the oxygen content at the metal surface, such estimates are indicated by the stippled lines in Figs. 2-4. As seen oxygen dissolution accounts for the main part of the weight gain observed. In the above estimates the diffusion coefficient has been assumed independent of oxygen concentration. In reality the oxygen diffusion is in all probability a function of the oxygen concentration, and the estimates are thus correspondingly approximate.

During the initial periods at the lower temperatures (<450 °C), i.e. during the logarithmic oxidation, the weight gain is appreciably higher than that estimated on the basis of oxygen dissolution alone. The question thus arises as to the mechanism of oxidation during the logarithmic oxidation.

5.2 Logarithmic oxidation. During the logarithmic oxidation oxygen dissolution and formation of metallic oxide phases take place. There is no evidence of formation of Ta_2O_5. This does not necessarily exclude the possibility of a very thin film of amorphous Ta_2O_5 on the surface as has been postulated by Vermilyea23) in studies of oxidation of tantalum at 50° - 300 °C. One might, however, ask what an amorphous film of Ta_2O_5 really means. Is it a more or less random or ordered arrangement of tantalum and oxygen atoms on the surface in the ratio 2:5? What crystal structure does this random or ordered arrangement take on when crystallizing? The diffraction studies show that the crystalline oxide phases which are formed consist of the metallic oxide phases.- The subsequent discussion will only be based on the results of the experimental studies without recourse to an assumption of presence of an amorphous film of Ta_2O_5 on the surface.

On the basis of the experimental results the oxidation is interpreted to involve the following steps:

$$Ta + O_{chem} \longrightarrow \begin{matrix}\text{Ta-O solid sol'n}\\ TaO_y\end{matrix} \longrightarrow TaO_z \qquad (2)$$

A rate-determining oxygen dissolution in the metal results in an approximate parabolic oxidation and thus do not explain the observed logarithmic behaviour. As discussed above the observed weight gain during logarithmic oxidation is furthermore appreciably higher than that expected on the basis of oxygen dissolution alone. It is consequently concluded that the logarithmic oxidation is associated with the formation of metallic oxide phases, and that this process is the predominating part-process during logarithmic oxidation.

Several theories based on various hypothetical rate-determining mechanisms have been put forward to explain logarithmic oxidation of metals. These theories include the tunnel-effect theory by Mott[38)], the electron-emission theory by Uhlig[39)], the chemisorption theory by Landsberg[40)], the disarray theory by Davies, Evans and Agar[41)], and the cavity theory by Evans[42)]. A summary of the important features of these theories has recently been given by Hurlen[43)]. In general all these theories presuppose formation of thin oxide films on the metal surface. The present experimental results do not indicate that this condition is met in logarithmic oxidation of tantalum. Rather, the formation of the metallic oxide phases takes place in the form of a regular pattern of individually isolated oxide platelets. TaO_z grows parallell to the $\{320\}$ sets of planes of the metal. The formation of oxide platelets furthermore appear to be favoured by grain boundaries and the presence of strain in the metal. The number of platelets are also found to vary considerably from grain to grain due to different orientations of the grains. On the basis of these considertions it is not unlikely that the logarithmic oxidation is associated with the nucleation and growth of the metallic oxide phases.

If the rate of oxidation under these conditions is assumed proportional to the rate of nucleation and growth of the oxide phase, this may be written:

$$\frac{dw}{dt} = K_o e^{-E/RT} \qquad (3)$$

where $\frac{dw}{dt}$ denotes the rate of oxidation and E the activation energy. The ease of nucleation of oxide will vary over the surface of the specimen due to different orientation of the grains, stresses and strain in the metal, presence of impurities, grain boundaries, defects in the metal, etc. The initial oxide nucleation will take place at the energetically most favorable sites. Subsequent nucleation will take place at less favorable sites, i.e. the activation energy of nucleation will increase with the number of nuclei formed. If one assumes that E increases linearly with w, E becomes

$$E = E_o + aw \qquad (4)$$

where a is a constant. Using this value of E, integration of Eq. 3 yields

$$w = \frac{RT}{a} \ln (t + t_o) - \frac{1}{a} (E_o + \ln t_o) \qquad (5)$$

where $t_o = \frac{RT}{aK_o}$. From Eq. 5 it is seen that w is proportional to the logarithm of time. Furthermore, the logarithmic rate constant, $K_{\log} = \frac{RT}{a}$, varies linearly with temperature.

As a test of the proposed oxidation mechanism the experimentally observed values of the logarithmic rate constant have been plotted as a function of temperature. This is shown in Fig. 23. As seen the results suggest a straight line relationship in accord with Eq.5. A usual Arrhenius plot of the logarithm of the rate constant as a function of reciprocal absolute temperature does not yield a straight-line relationship, but one obtains a curve which is concave downwards.

It must of course be emphasized that Eqs. 4 and 5 are not valid for large values of w. The above treatment is only proposed to be applicable for initial oxidation with only partial oxide coverage of the metal surface. After prolonged oxidation with full oxide coverage of the surface one of several mechanisms of oxidation may be expected to be applicable. In such cases the rate of transport of ions through the oxide or along grain boundaries may be rate determining. If the rate of nucleation and growth of oxide still is rate-determining, one will expect an average steady-state value for E with a consequent linear oxidation according to Eq. 3.

Studies in recent years of low-temperature and low-pressure oxidation of metals has to an increasing extent shown the great importance of oxide nucleation and growth of oxide nuclei in the oxidation reaction. Low-temperature oxidation of metals in general shows logarithmic type behaviour, and it is suggested that the same general considerations as discussed above for tantalum may be applicable to other metals.

The experimental results suggest that the initial oxidation at the lower temperatures is oxygen-pressure dependent. At the lower oxygen pressures the oxidation may no longer be described by a logarithmic type behaviour and it is not possible to assign a definite rate equation for the oxidation. Consequently it is not possible to give an analytical description of the oxygen pressure dependence. Qualitatively the oxygen pressure dependence is interpreted in terms of an oxygen chemiscrption equilibrium prior to the nucleation and growth of the metallic oxide nuclei. The consentration of chemisorbed oxygen atoms may qualitatively be expected to markedly influence the rate of initial oxide nucleations. However, at present it is difficult to evaluate these effects, the elucidation of which will require detailed studies of the oxidation of well-defined crystal surfaces.

5.3 Approximate parabolic oxidation. Considering oxidation over longer periods of time at the lower temperatures it is found that the oxidation proceeds faster than that of a logarithmic oxidation. Under these conditions it is again difficult to assign a clear-cut rate equation to the results, but after extended periods the oxidation may be described as approximately parabolic. The initial oxidation at the higher temperatures may also be described by the same relationship (Figs. 3 and 5 b).

In this connection it may also be important to note that a double-logarithmic plot of the results (Fig. 3) also suggest conformity with an approximate cubic oxidation over periods of time. However, it is often dangerous to infer rate equations from double logarithmic plots, and the cubic oxidation is in the present case only believed to reflect concurrent logarithmic and parabolic part-processes. It is easily shown that a combination of two such processes may lead to approximate cubic oxidation rates over periods of time.

In the parabolic region the oxidation constitutes oxygen dissolution and formation of the metallic oxide phases TaO_y and TaO_z. However, as shown above, under these conditions oxygen dissolution accounts for the main part of the observed weight gain. The transition from a logarithmic to an approximate parabolic oxidation, is consequently interpreted as being due to the fact that with increasing time the relative importance of oxygen dissolution increases and that it eventually becomes the main rate-determining process.

Oxygen diffusion has a larger temperature dependence than that of the logarithmic oxidation. This in turn means that oxygen dissolution also becomes of increasing relative importance with increasing temperature. Thus with increasing temperature the duration of the logarithmic period becomes shorter and eventually no longer is of any importance. This qualitatively explains that the initial oxidation at the higher temperatures follows an approximate parabolic oxidation.

An Arrhenius plot of the results in Fig. 5 b gives a straight-line relationship at 350° to 450 °C with an activation energy of $29^{kcal}/mole$ (k_{par} expressed in $mg^{-2}cm^{-4}min^{-1}$). Above 450 °C an increased activation energy is observed. Corresponding studies by Gulbransen and Andrew[19,20] at 250° to 450 °C gave an activation energy of $27.4^{kcal}/mole$ for the parabolic oxidation. In terms of the above interpretation this activation energy should correspond to an average value of the activation energy for oxygen diffusion in tantalum-oxygen solid solutions. At an oxygen concentration of 1 at%

this activation energy has been found to be 27.7 kcal/mole by means of internal friction methods. The close agreement in activation energies further confirms the proposed interpretations.

In the above discussion the oxidation mechanism has been simplified by considering the oxygen dissolution and metallic oxide formation as separate and concurrent part-processes. In reality these processes are interrelated. The nucleation of the metallic oxide phases in the form of oxide platelets extending into the metal will be a function of the oxygen concentration in the metal. Similarly, during nucleation of the oxide phase from a supersaturated tantalum-oxygen solid solution, a decrease in the oxygen concentration in the metal immediately surrounding the oxide phase will take place. This decrease in oxygen concentration will in turn increase the rate of diffusion of oxygen in this part of the metal. Thus the oxidation mechanism will involve an interplay between oxygen dissolution and formation of the metallic oxide phases. With increasing temperature one will furthermore expect greater ease of growth of the oxide phase. Thus with increasing temperature the initial approximate parabolic oxidation will be expected to involve formation of increased amounts of the metallic oxide phases in addition to the oxygen dissolution effects. These effects and their interplay are concluded to cause the increase in activation energy of the initial approximate parabolic oxidation above 450 °C.

54 Breakaway oxidation. The breakaway oxidation is found to be associated with Ta_2O_5 formation. During the initial transition to the breakaway oxidation the first traces of Ta_2O_5 in spots and local areas on the surface are observed, while during breakaway oxidation heavy Ta_2O_5-formation is found. The Ta_2O_5 has little or no protective properties as evidenced by the many blisterlike and "volcanic" ruptures of the oxide scale. The metallographic studies indicate that the Ta_2O_5 is formed on or at the metallic oxide phase TaO_z. The incubation period until the transition to the breakaway oxidation is found to decrease with increasing temperature.

The breakaway oxidation of tantalum has been discussed in greater detail in a previous publication1), and only a short summary will be given here. The previous studies were carried out on cold-rolled Ta-specimens with a thickness of 1.5 mm, while the present studies were made on cold-rolled specimens of 0.1 to 0.3 mm thickness. Within the limits of error no difference in oxidation behaviour during breakaway oxidation was observed between the specimens of different thicknesses. The thinner specimens of course becomes saturated with oxygen at a much earlier time than the thicker specimens, and only due to such effects - after more extended oxidation - are marked differences observed.

As shown and discussed elsewhere1) the linear, breakaway oxidation is interpreted in terms of a rate-determining nucleation and growth of Ta_2O_5-nuclei. The rate-determining step is preceded by an oxygen chemisorption equilibrium. The linear rate constant is given by the expression

$$k_1 = \frac{ak\,Kp_{O_2}^{1/2}}{(RT)^{1/2} + Kp_{O_2}^{1/2}} \qquad (6)$$

where a represents the number of chemisorption sites, k the rate-determining constant for the nucleation and growth of oxide nuclei, and K the chemisorption equilibrium constant. ak is given by the relationship $ak = 1.7 \times 10^{17} \exp(- \frac{71100}{RT})$, while the heat of chemisorption of 1/2 mole of oxygen is 64.4 kcal. At low temperatures and high oxygen pressures Eq. 6 reduces to

$$k_1 = ak \qquad (7)$$

e.g. the rate of breakaway oxidation becomes approximately independent of oxygen pressure.

At high temperatures and low pressures Eq. 6 takes the form

$$k_1 = \frac{ak\, Kp_{O_2}^{1/2}}{(RT)^{1/2}} \qquad (8)$$

i.e. the oxidation is approximately proportional to $p_{O_2}^{1/2}$.

The logarithm of the duration of the incubation period for the breakaway oxidation has been found approximately proportional to reciprocal absolute temperature and has interpreted in terms of the time lag associate with the diffusion and rearrangement of atoms during nucleation and growth of the Ta_2O_5 nuclei[1)]. Part of this time lag is also due to the time associated with oxygen dissolution and formation of TaO_2. This latter time lag is, however, short compared to that of the Ta_2O_5-formation.

Eqs. 6-8 may be used to estimate the rate of Ta_2O_5-formation at lower temperatures. Extrapolation of Eq. 6 (or 7) suggests a linear rate for the "breakaway" oxidation of $1.25 \cdot 10^{-6}$ mg cm^{-2}min^{-1}at 400 °C and 1 atm. O_2. This rate is more than a factor of 10 lower than the observed rate of oxidation after 3000 min at 400 °C which may be estimated to $2 \cdot 10^{-5}$ mg cm^{-2}min^{-1} (Fig. 3). Thus the rate of oxygen dissolution and formation of the metallic oxide phases is more than 10 times faster than the Ta_2O_5-formation under these conditions. A corresponding extrapolation to 400 °C suggests an incubation period for the "breakaway" oxidation of 20 000 min at this temperature[1). This explains the absence of Ta_2O_5 at 400 °C and lower temperature in the presently employed experimental conditions.

During the breakaway oxidation oxygen dissolution into the metal, of course , continues to take place. However, in reaction rate studies at the highest temperatures and oxygen pressures the weight gain due to Ta_2O_5- formation is in general much higher than the weight gain due to dissolved oxygen. Thus oxygen dissolution may in such cases be considered of minor importance in the reaction kinetics.

ACKNOWLEDGEMENT

The work has been sponsored by the Metallurgy and Ceramics Research Branch, ARL, Office of Aerospace Research, United States Air Forse, monitored by the European Office, Office of Aerospace Research under Grant No. AF - EOAR - 61-42.

The author is indebted to Dr. N. Norman and Mr. O.J. Krudtaa for the x-ray diffraction and metallographic studies, respectively. Thanks are also due to the many members of this institute for their assistance in the various phases of the experimental studies.

REFERENCES

1) P. Kofstad, "Oxidation of Tantalum in the Temperature Tange 500-700 °C", Central Institute for Industrial Research, Oslo, Norway. Technical (Final) Report, Contract No. AF 61(052)-90. April 1961. To be published in J. Inst. Metals.

2) E. Gebhardt and H-D. Seghezzi; 3rd Plansee Seminar, Reutte, Austria (1958), p. 280.

3) H-D. Seghezzi, Zeitschrift für Metallkunde; (1959) 248, 521.

4) R.J. Wasilewski; J.A.C.S., 75 (1953) 1001.

5) N. Schöberg; Acta Chem. Scand., 8 (1954) 240.

6. C.Y. Ang; Acta Met., 1 (1953) 123.

7) T.W. Marx, G.S. Baker. and J.M. Sivertsen: Acta Met., 1 (1953) 193.

8) R.W. Powers; Acta Met., 3 (1955) 135.

9) R.W. Powers and M.V. Doyle, Acta Met. 4 (1956) 233.

10) R.W. Powers and M.V. Doyle; Trans. AIME, 215 (1959) 655.

11) R.W. Powers and M.V. Doyle; J. Appl. Phys. 30 (1959) 514.

12) E. Gebhardt, H-D. Seghezzi, and A. Stegherr, Zeitschrift f. Metallkunde, 48 (1957) 624.

13) G. Brauer and H. Müller, 3rd Plansee Seminar, p. 257, Vienna 1959.

14) G.L. Miller, "Tantalum and Niobium", Butterworth Scientific Publications, London, 1959.

15) J.V. Cathcart and R.F. Pawel, private communications.

16) N. Norman, "Metallic Oxide Phases of Niobium and Tantalum. X-ray Investigations", Central Institute for Industrial Research, Oslo, Norway, Grant AF EOAR 61-42, TN No. 1., October 1961. To be published in J. Less Common Metals.

17) N. Norman, P. Kofstad, and O.J. Krudtaa. "Metallic Oxide Phases of Niobium and Tantalum. Metallographic Studies". Central Institute for Industrial Research, Oslo, Norway, Grant AF EOAR 61-42, TN No. 2, October 1961. To be published in J. Less Common Metals.

18) S. Lagergren and A. Magneli, Acta Chem. Scand., 6 (1952) 444.

19) E.A. Gulbransen and K.F. Andrew, Trans AIME, 188 (1950) 586.

20) E.A. Gulbransen and K.F. Andrew, J. Electrochem. Soc. 96 (1949) 364.

21) R.C. Peterson, W.M. Fassell, Jr., and M.E. Wadsworth, J. Metals 6 (1954) 1038.

22) R. Bakish, J. Electrochem. Soc. 105 (1958) 574.

23) D.A. Vermilyea, Acta Met. 6 (1958) 166.

24) K. Hauffe, Z.f.Electrochemie, Ber. Bunsengesellschaft f. Phys. Chem. 63 (1959) 819.

25) R. Bakish, J. Electrochem. Soc. 105 (1958) 71.

26) M.G. Cowgill and J.Stringer, J. Less Common Met. 2 (1960) 233.

27) J.T. Waber, G.E. Sturdy, E.M. Wise and C.R. Tipton, J. Electrochem. Soc. 99 (1952) 121.

28) J.T. Waber, J. Chem. Phys., 20 (1952) 735.

29) J.V. Cathcart, R. Bakish, and D.R. Norton, J. Electrochem. Soc. 107 (1960) 668.

30) J.V. Cathcart, private communications.

31) R.E. Pawel, J.V. Cathcart, and J.J. Campbell, J. Electrochem. Soc. 107 (1960) 956.

32) W.M. Albrecht, W.D. Klopp, B.G. Koehl, and R.I. Jaffee, Trans. AIME, (1961).

33) T. Hurlen, H. Kjöllesdal, J. Markali, and N. Norman, "Oxidation of Niobium", ARDC Technical Note No. 1, No. AF 61(052)-90, Central Institute for Industrial Research, Oslo, Norway, April 1959.

34) P. Kofstad, H. Kjöllesdal, J. Markali, and N. Norman, "High-Temperature Oxidation of Niobium" ARDC Technical Note No. 2, No. AF 61(052)-90, Central Inst. for Ind. Res., Oslo, Norway, April 1960.

35) O.J. Krudtaa and K. Stokland, Metal Progress, 77 (1960) 101.

36) P. Kofstad and O.J. Krudtaa, to be published

37) L.S. Darken and R.W. Gurry, "Pysical Chemistry of Metals", McGraw-Hill, New York, (1953), p. 445.

38) N.F. Mott, Trans. Faraday Soc., 35 (1939) 1175.

39) H.H. Uhlig, Acta Met., 4 (1956) 541.

40) P.T. Landsberg, J. Chem. Phys. 23 (1955) 1079.

41) D.E. Davies, U.R. Evans and J.N. Agar, Proc. Roy. Soc. [A] 225 (1954) 443.

42) U.R. Evans, Rev. Pure and Appl. Chem. 5 (1955) 1.

43) T. Hurlen , J. Inst. Metals, 89 (1960) 128.

LIST OF ILLUSTRATIONS

Fig. 10a. Surface of highvacuum annealed Ta-specimen oxidized for 300 min. at 400 °C and 1 atm. oxygen. 500 x.

Fig. 10b. Surface of highvacuum annealed Ta-specimen oxidized for 300 min. at 400 °C and 1 atm. oxygen. 500 x.

Fig. 11. Surface of specimen shown in Fig. 10a and b after polishing and etching. 1250 x.

Fig. 12a. Surface of high-vacuum annealed Ta-specimen oxidized for 300 min. at 500 °C and 10 torr oxygen. 100 x.

Fig. 12b. Surface of high-vacuum annealed Ta-specimen oxidized for 300 min. at 500 °C and 10 torr oxygen. 500 x.

Fig. 12c. Surface of high-vacuum annealed Ta-specimen oxidized for 300 min. at 500 °C and 10 torr oxygen. 100 x.

Fig. 12d. Surface of high-vacuum annealed Ta-specimen oxidized for 300 min. at 500 °C and 10 torr oxygen. 500 x.

Fig. 13. Specimen shown in Fig. 12 after polishing and etching. 500 x.

Fig. 14. Specimen in Fig. 12 after polishing and etching. 1250 x.

Fig. 15. High-vacuum annealed Ta-specimen oxidized for 400 min. at 500 °C and 10 torr oxygen. Oxidized surface polished and etched resulting in partial removal of Ta_2O_5 on surface. 250 x.

Fig. 16. High-vacuum annealed Ta-specimen oxidized for 1300 min. at 600 °C and 10^{-2} torr oxygen. Surface polished and etched after oxidation. Platelets of TaO_2 with growth of Ta_2O_5 (dark grey).

Fig. 17. Electron micrograph (replica) of surface of cold-rolled and polished Ta-specimen oxidized for 3200 min. at 350 °C and 1 atm. oxygen. 6150 x.

Fig. 18. Electron micrograph (replica) of surface of cold-rolled and polished Ta-specimen oxidized for 300 min. at 450 °C and 1 atm. oxygen. 11600 x.

Fig. 19a. Electron micrograph (replica) of surface of cold-rolled Ta-specimen (polished and etched before oxidation) oxidized for 300 min. at 500 °C and 10 torr oxygen. 3550 x.

Fig. 19b. Electron micrograph (replica) of surface of high-vacuum annealed Ta-specimen (polished and etched before oxidation) oxidized for 300 min. at 500 °C and 10 torr oxygen. 3550 x.

Fig. 19c. Electron micrograph of surface of high-vacuum annealed Ta-specimen (polished and etched before oxidation) oxidized for 300 min. at 500 °C and 10 torr oxygen. 6000 x.

Fig. 20. Microindentation hardness as a function of distance from the metal surface. Cold-rolled and polished Ta-specimen oxidized for 3200 min. at 350 °C and 1 atm. oxygen.

Fig. 21. Microindentation hardness as a function of distance from the metal surface. Cold-rolled and polished Ta-specimens oxidized at 400 °C and 1 atm. oxygen.

Fig. 22. Microindentation hardness as a function of distance from the metal surface. Cold-rolled and annealed Ta-specimens oxidized for 300 min. at 500 °C and 10 torr oxygen.

Fig. 23. The rate constant for the logarithmic oxidation of tantalum as a function absolute temperature.

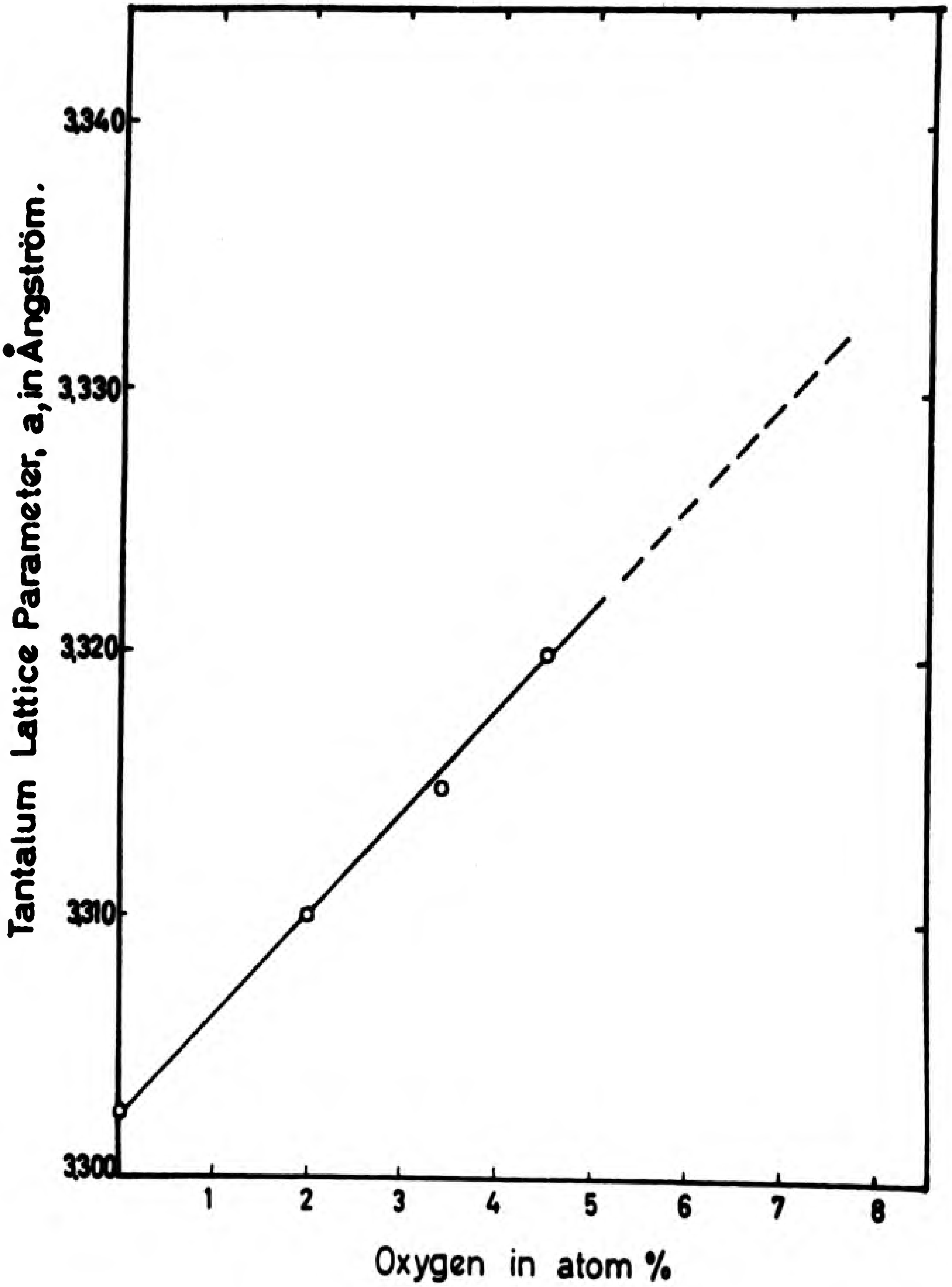

Fig. 1. The tantalum lattice parameter as a function of oxygen concentration. After Gebhardt and Seghezzi2).

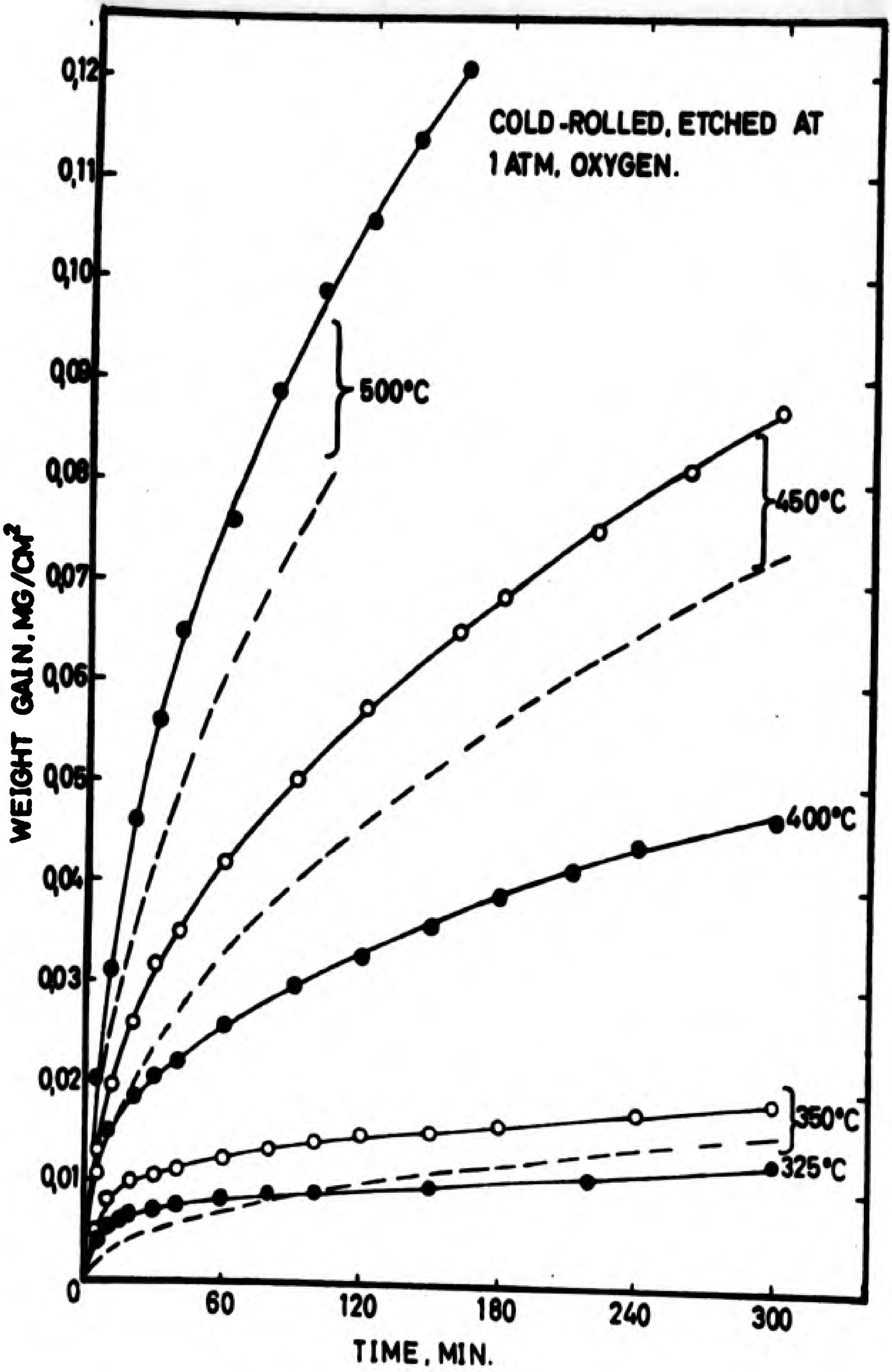

Fig. 2. Oxidation of cold-rolled tantalum (polished and etched) at temperatures 325° to 500 °C and 1 atm. oxygen. Weight gain as a function of time. Stippled lines indicate weight gain on the basis of oxygen dissolution alone.

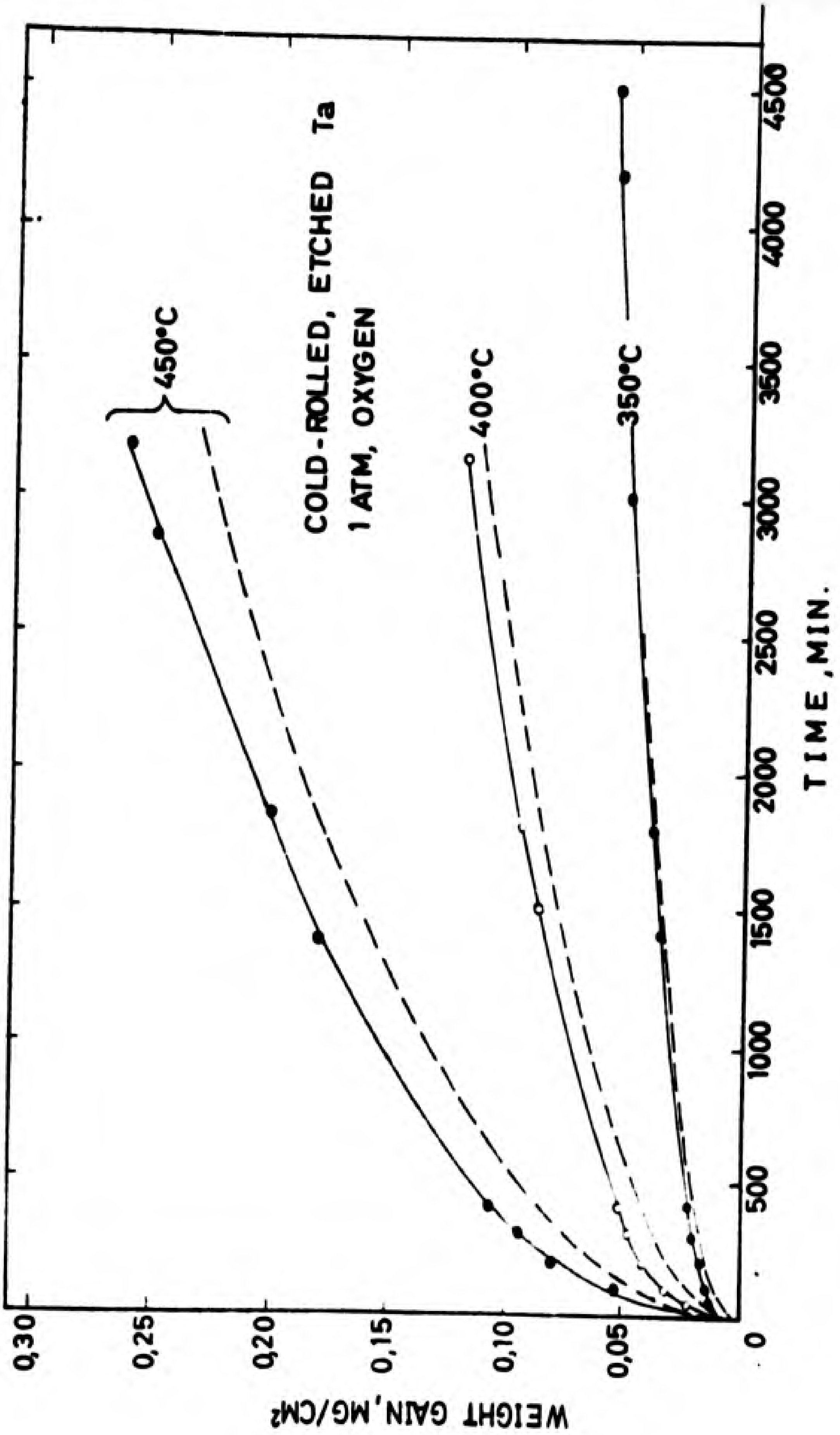

Fig. 3. Oxidation of cold-rolled tantalum (polished and etched) at temperatures 350° to 450 °C and 1 atm. oxygen. Weight gain as a function of time. Stippled lines indicate weight gain on the basis of oxygen dissolution alone.

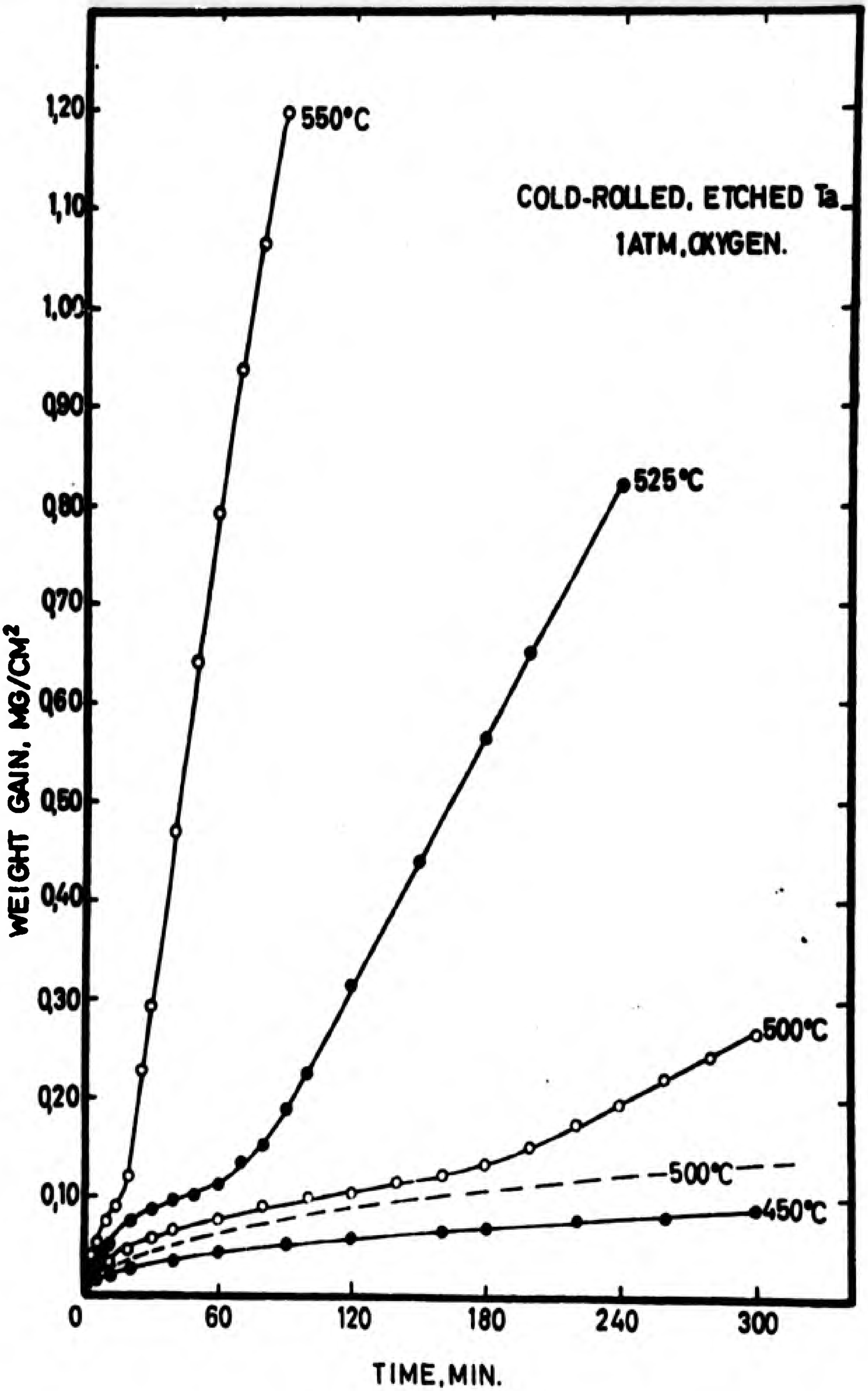

Fig. 4. Oxidation of cold-rolled tantalum (polished and etched) at temperatures 450° to 550 °C and 1 atm. oxygen. Weight gain as a function of time. Stippled lines indicate weight gain on the basis of oxygen dissolution alone.

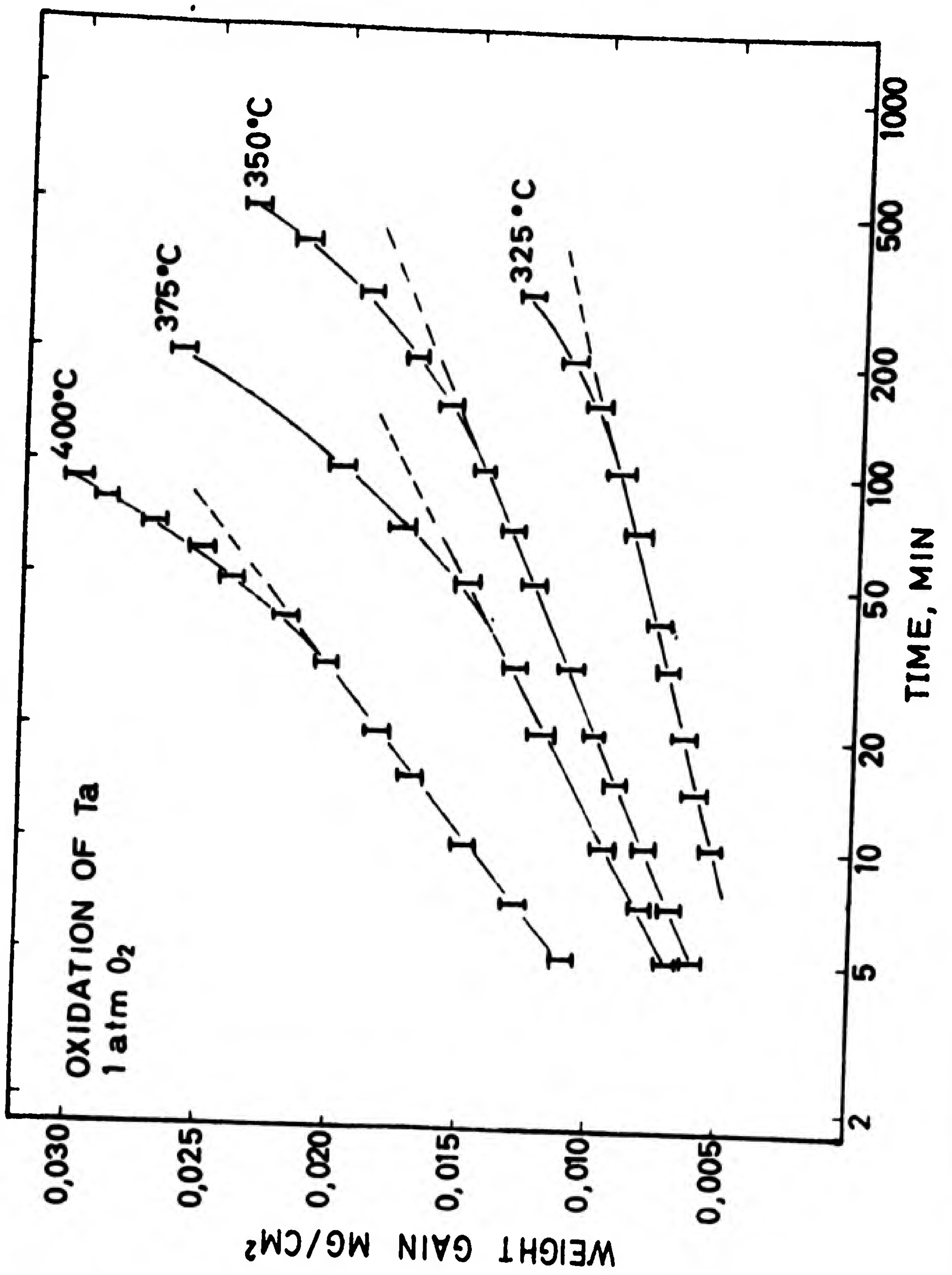

Fig. 5a. Oxidation of cold-rolled tantalum (polished and etched) at temperatures 325° to 400 °C at 1 atm. oxygen. Semi-logarithmic plot. Weight gain as a function of logarithm of time.

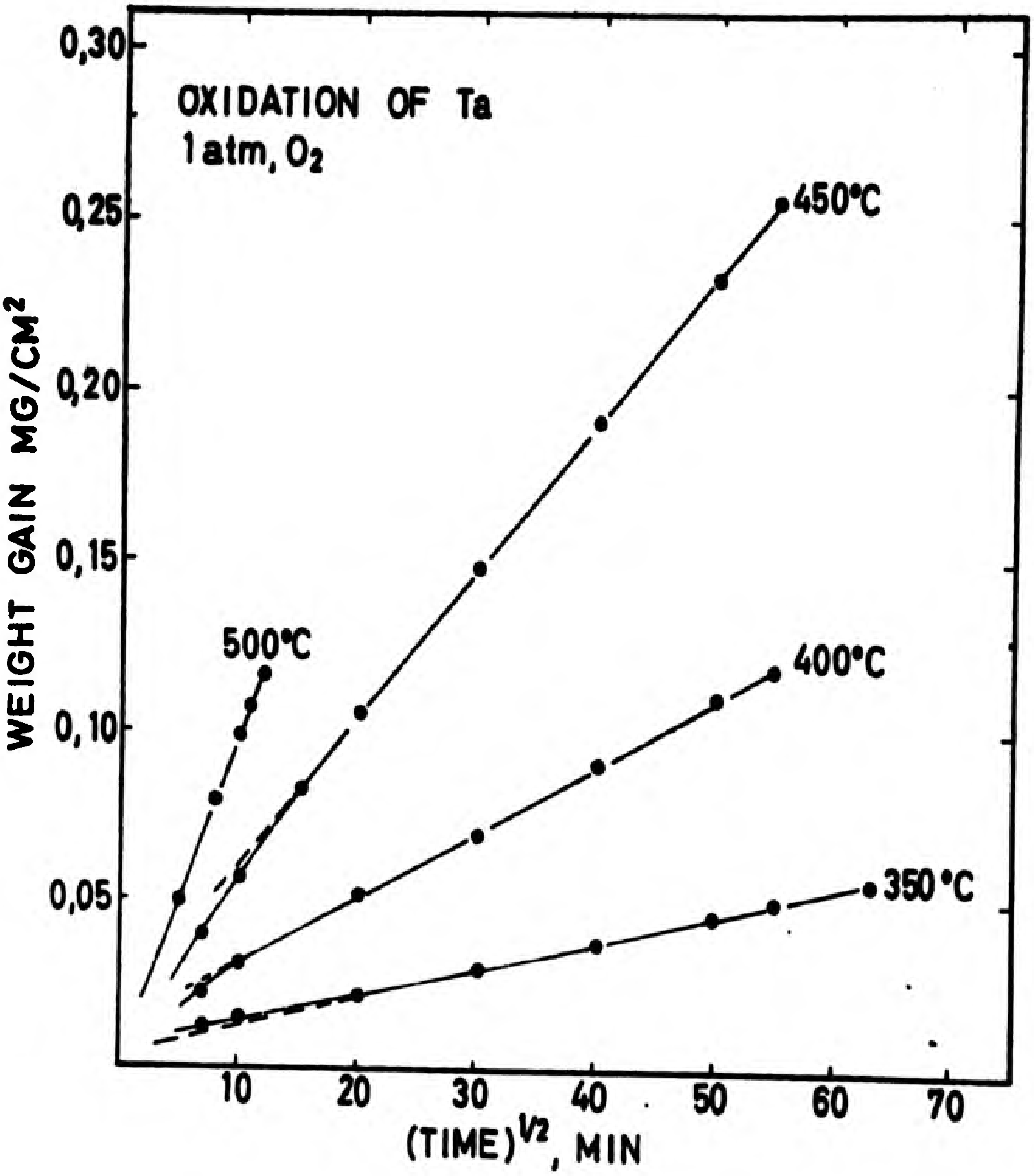

Fig. 5b. Oxidation of cold-rolled tantalum (polished and etched) at 350° to 500 °C and 1 atm. oxygen. Parabolic plot. Weight gain as a function of square root of time.

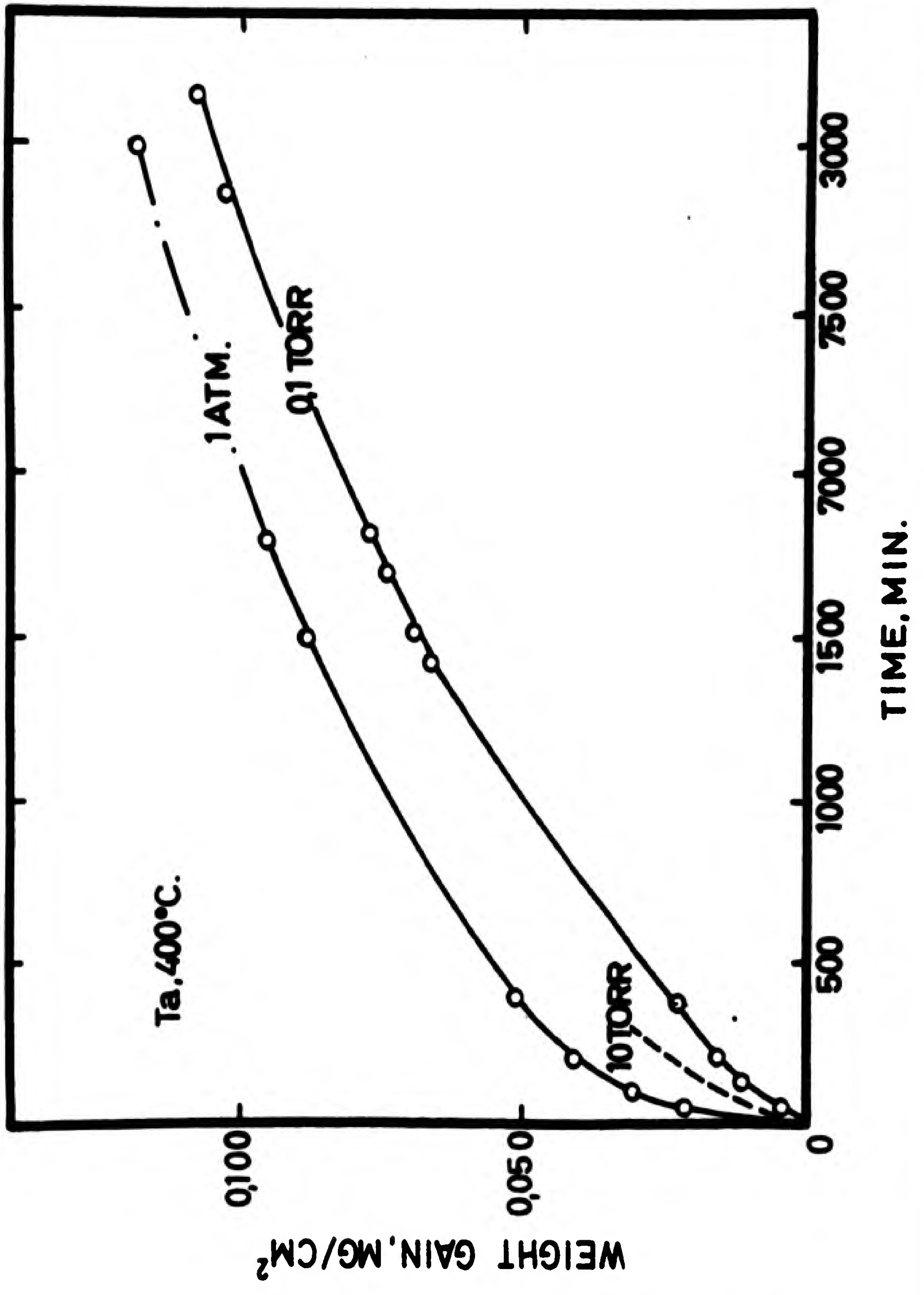

Fig. 6. Oxidation of cold-rolled tantalum (polished and etched) as a function of oxygen pressure at 400 °C. Weight gain as a function of time.

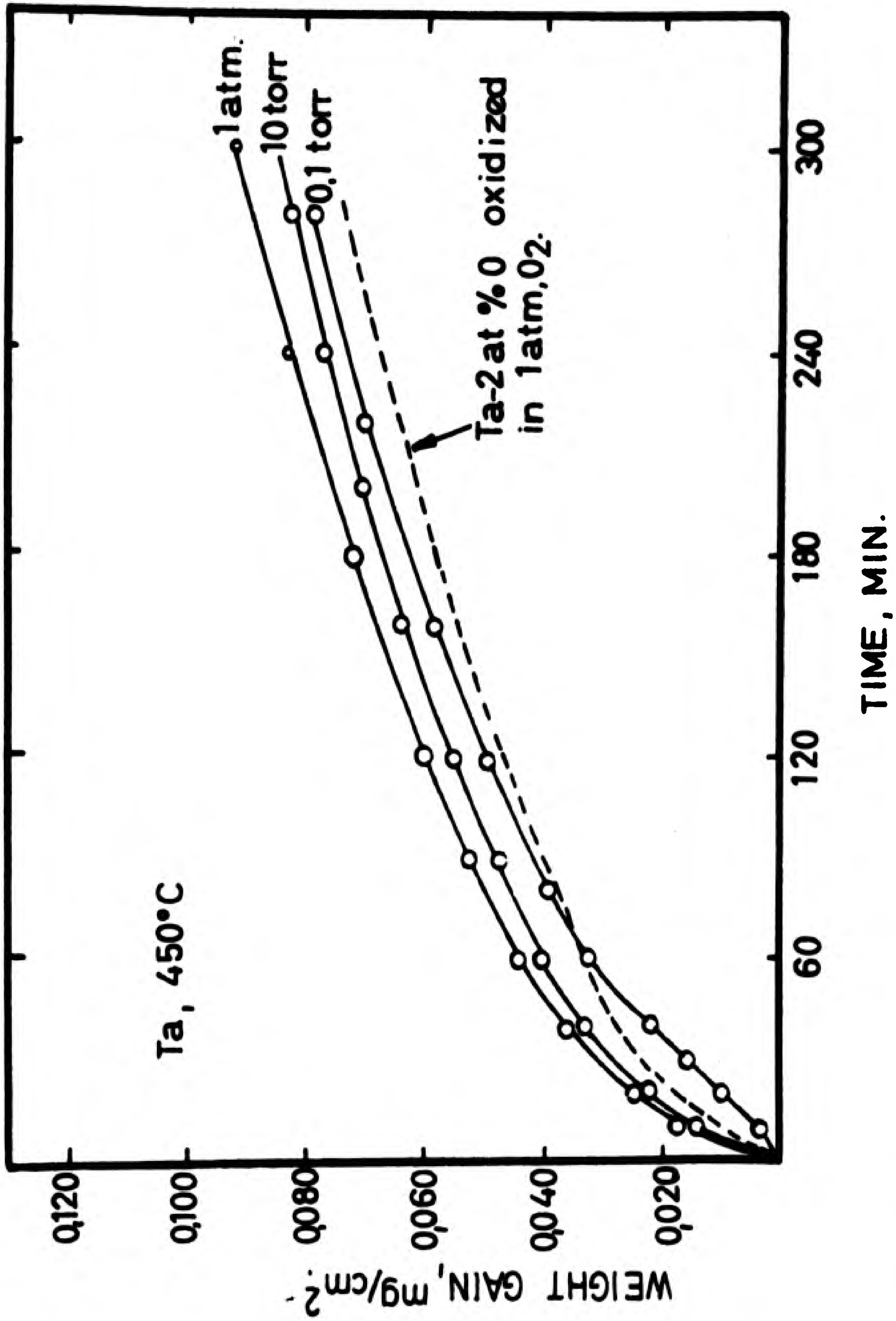

Fig. 7. Oxidation of cold-rolled tantalum (polished and etched) as a function of oxygen pressure at 450 °C. Weight gain as a function of time.

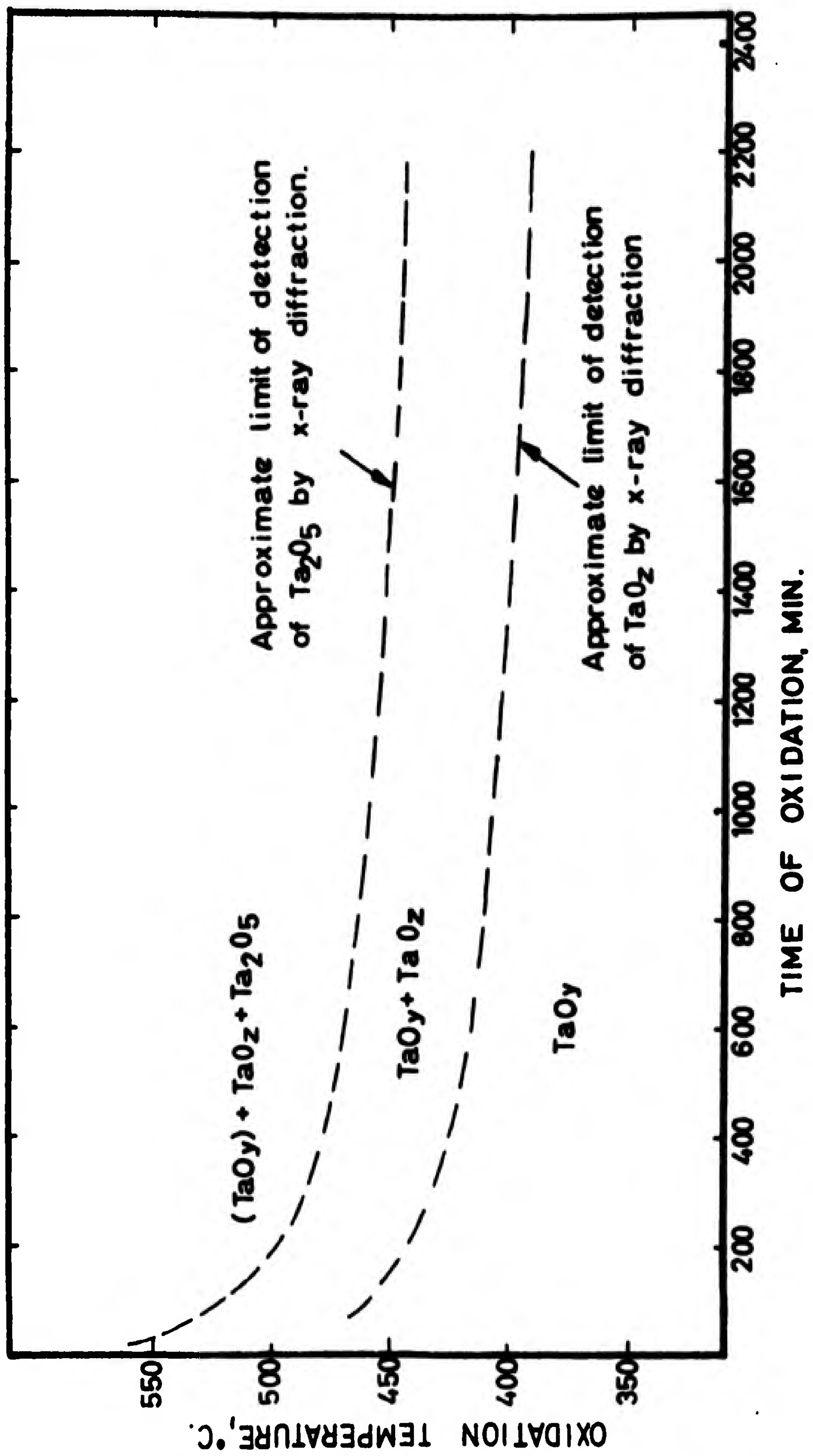

Fig. 8. Approximate limits of detection of TaO_z and Ta_2O_5 by x-ray diffraction as a function of temperature and time of oxidation.

Fig. 9.

Surface of cold-rolled Ta-specimen oxidized for 3200 min. at 350° C and 1 atm. oxygen. 1750 x.

Fig. 10 a.

Surface of high-vacuum annealed Ta-specimen oxidized for 300 min. at 400° C and 1 atm. oxygen. 500 x.

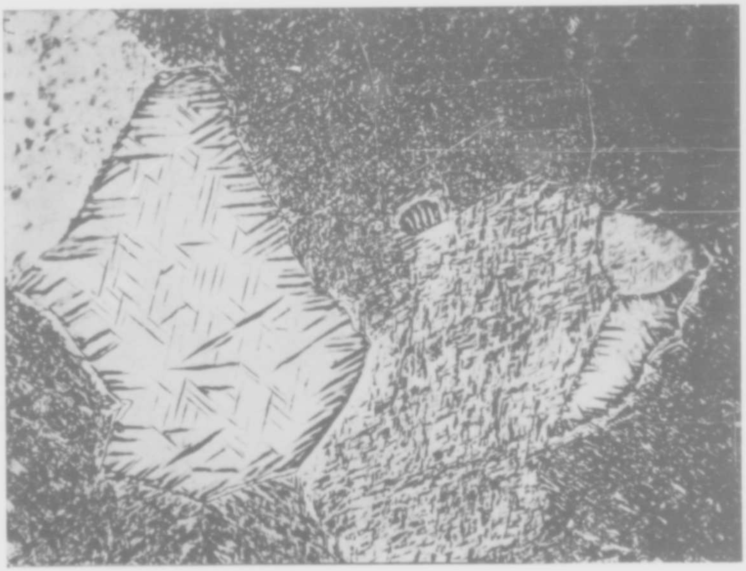

Fig. 10 b.
Surface of high-vacuum annealed Ta-specimen oxidized for 300 min. at 400° C and 1 atm. oxygen. 500 x.

Fig. 11.
Surface of specimen shown in Fig. 10 b after metallographic polishing and etching. 1250 x.

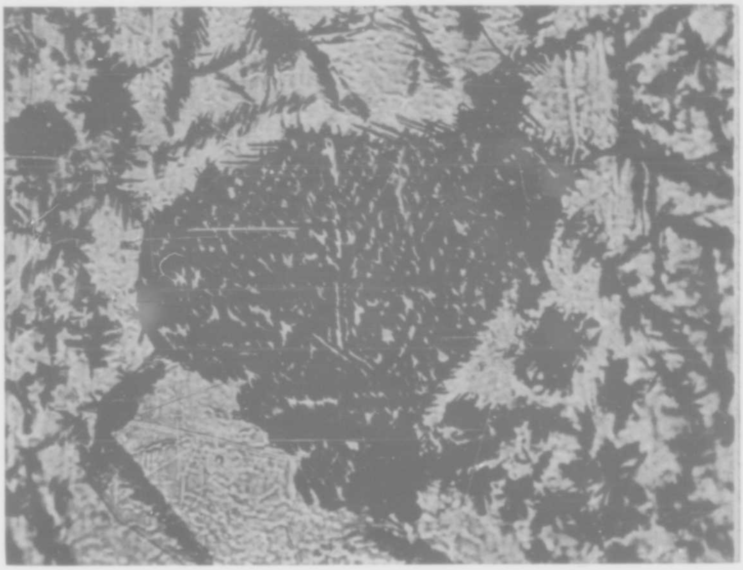

Fig. 12 a.
Surface of high-vacuum annealed Ta-specimen oxidized for 300 min. at 500° C and 10 torr oxygen. 500 x.

Fig. 12 b.
Surface of high-vacuum annealed Ta-specimen oxidized for 300 min. at 500° C and 10 torr oxygen. 500 x.

Fig. 12 c.

Surface of high-vacuum annealed Ta-specimen oxidized for 300 min. at 500° C and 10 torr oxygen. 100 x.

Fig. 12 d.

Surface of high-vacuum annealed Ta-specimen oxidized for 300 min. at 500° C and 10 torr oxygen. 500 x.

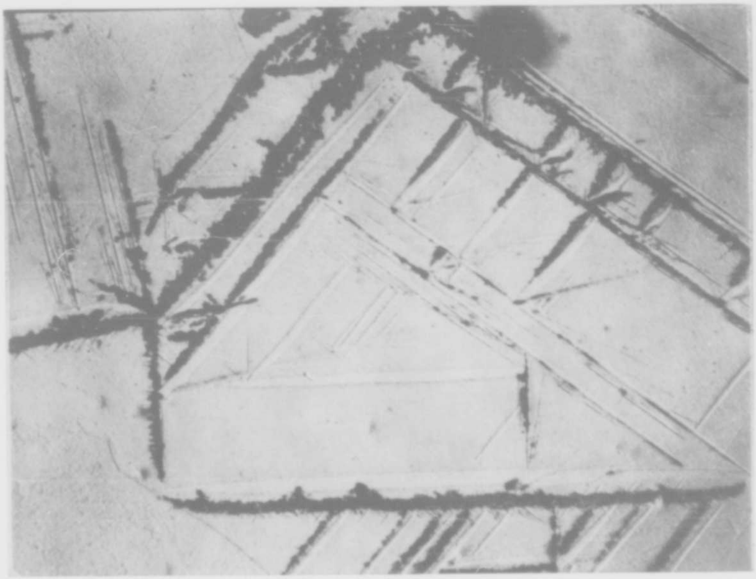

Fig. 13.

Specimen shown in Fig. 12 after metallographic polishing and etching. 500 x.

Fig. 14.

Specimen in Fig. 12 after metallographic polishing and etching. 1250 x.

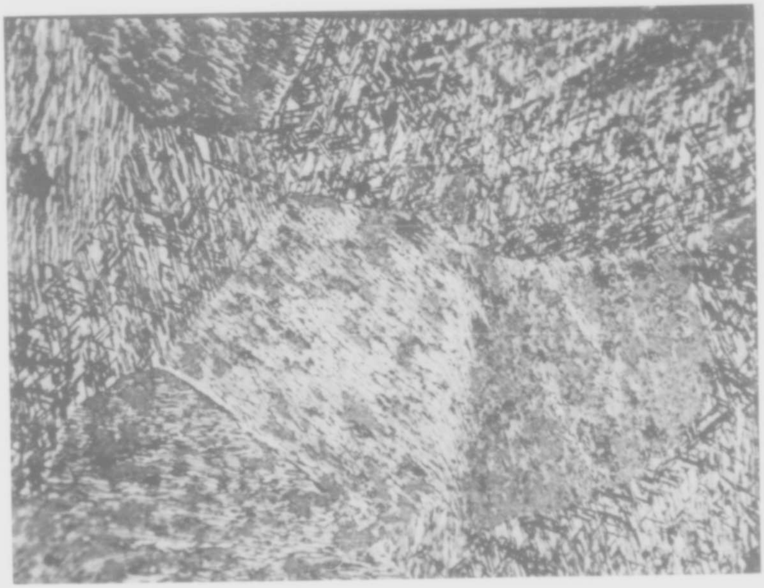

Fig. 15.

High-vacuum annealed Ta-specimen oxidized for 400 min. at 500° C and 10 torr oxygen. Oxidized surface metallographically polished and etched resulting in partial removal of Ta_2O_5 on surface. 500 x.

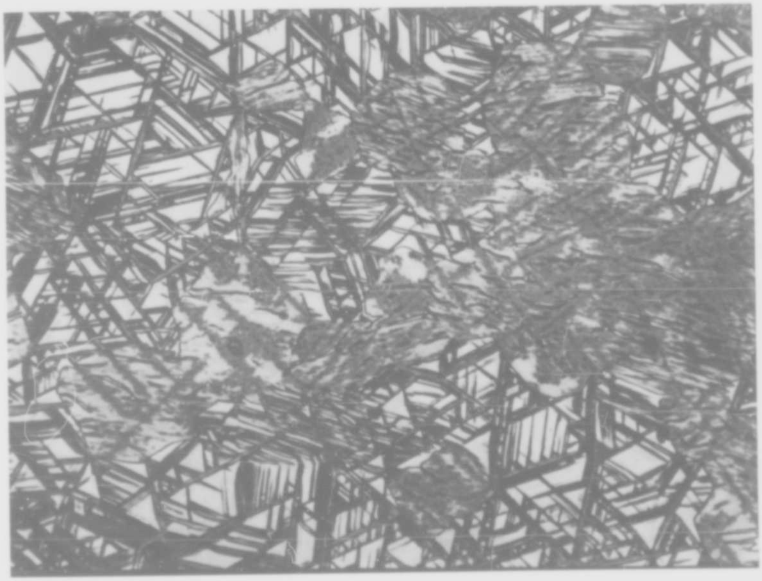

Fig. 16.

High-vacuum annealed Ta-specimen oxidized for 1300 min. as 600° C and 10^{-2} torr oxygen. Surface metallographically polished and etched after oxidation. Platelets of TaO_2 with growth of Ta_2O_5 (dark grey). 250 x.

Fig. 17.

Electron micrograph (replica) of surface of cold-rolled and polished Ta-specimen oxidized for 3200 min. at 350° C and 1 atm. oxygen. 6150 x

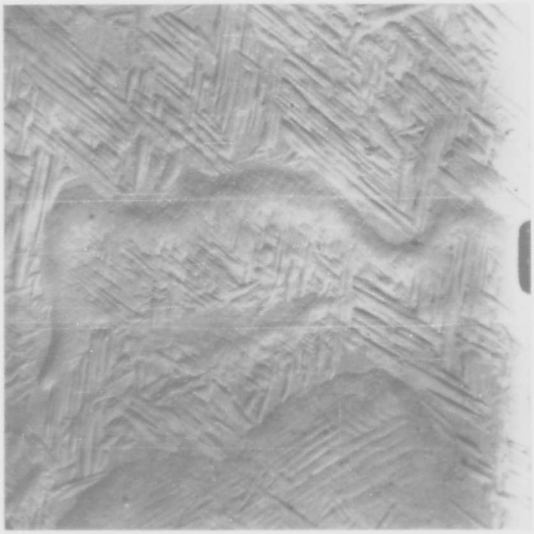

Fig. 18.

Electron micrograph (replica) of surface of cold-rolled and polished Ta-specimen oxidized for 300 min. at 450° C and 1 atm. oxygen. 11600 x.

Fig. 19 a.
Electron micrograph (replica) of surface of coldrolled Ta-specimen (polished and etched before oxidation) oxidized for 300 min. at 500° C and 10 torr oxygen. 3550 x.

Fig. 19 b.
Electron micrograph (replica) of surface of high-vacuum annealed Ta-specimen (polished and etched before oxidation) oxidized for 300 min. at 500° C and 10 torr oxygen. 3550 x.

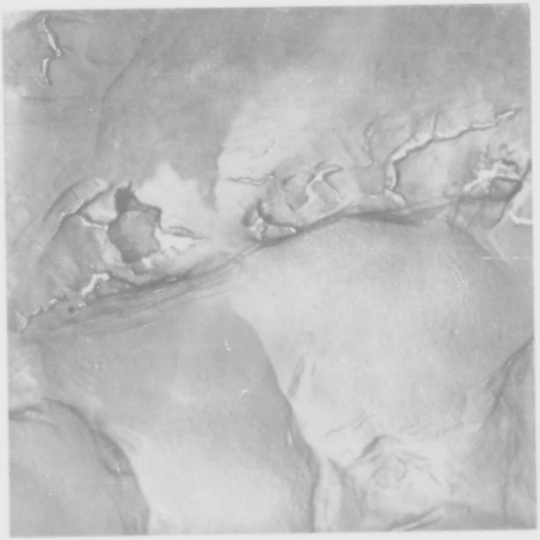

Fig. 19 c.
Electron micrograph (replica) of surface of high-vacuum annealed Ta-specimen (polished and etched before oxidation) oxidized for 300 min. at 500° C and 10 torr oxygen. 6000 x.

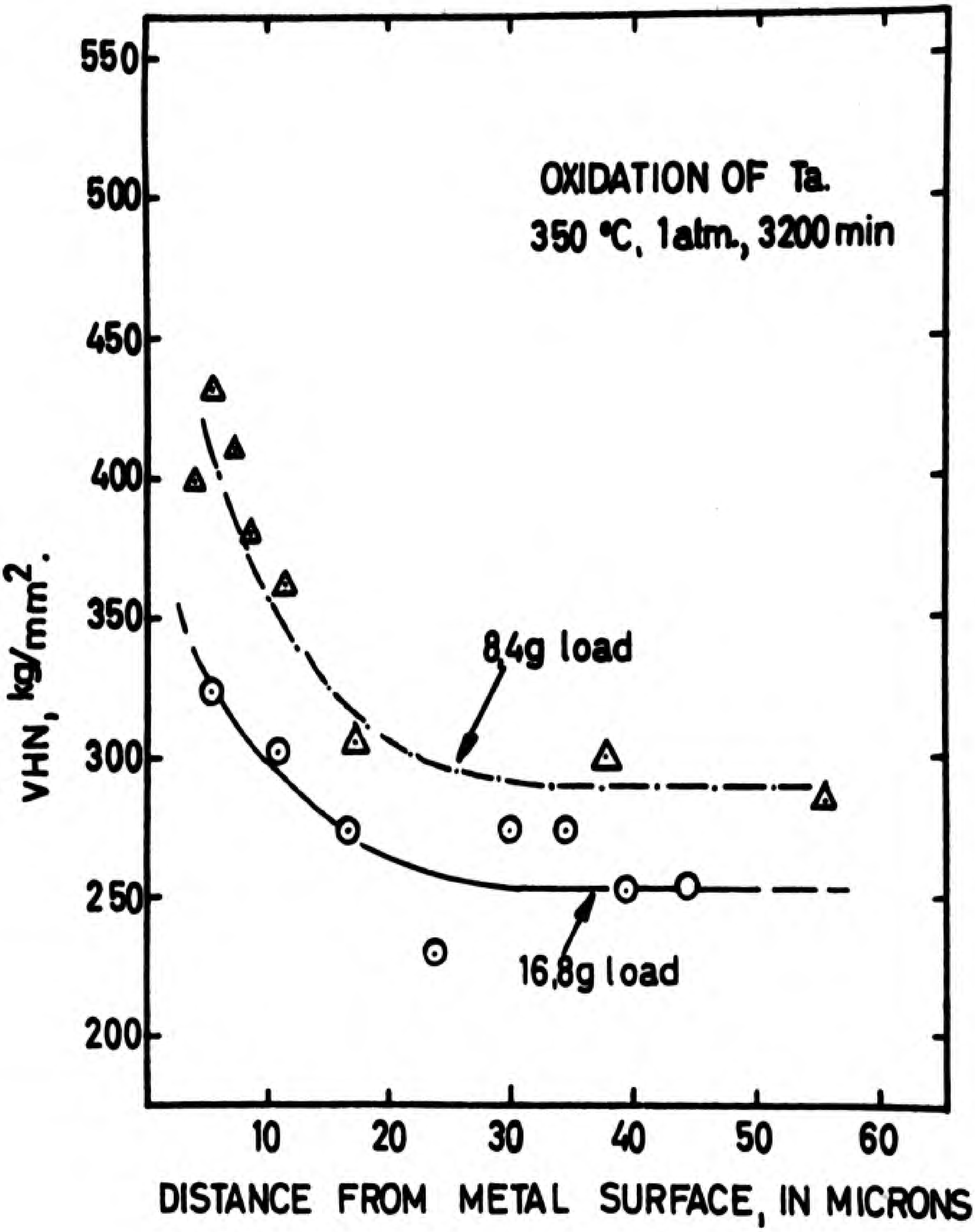

Fig. 20. Microindentation hardness as a function of distance from the metal surface. Cold-rolled and polished Ta-specimens oxidized for 3200 min. at 350 °C and 1 atm. oxygen.

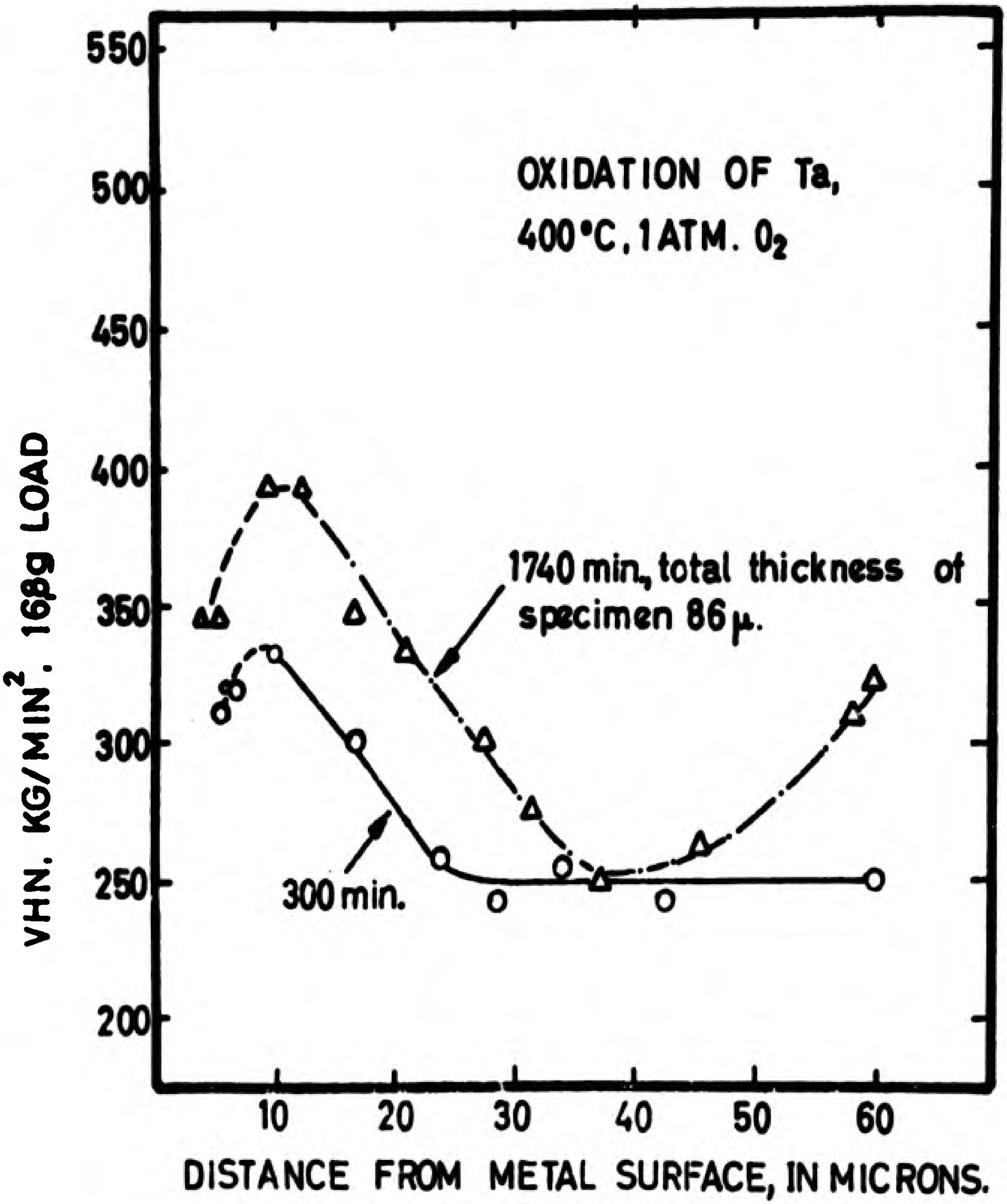

Fig. 21. Microindentation hardness as a function of distance from the metal surface. Cold-rolled and polished Ta-specimens oxidized at 400 °C and 1 atm. oxygen.

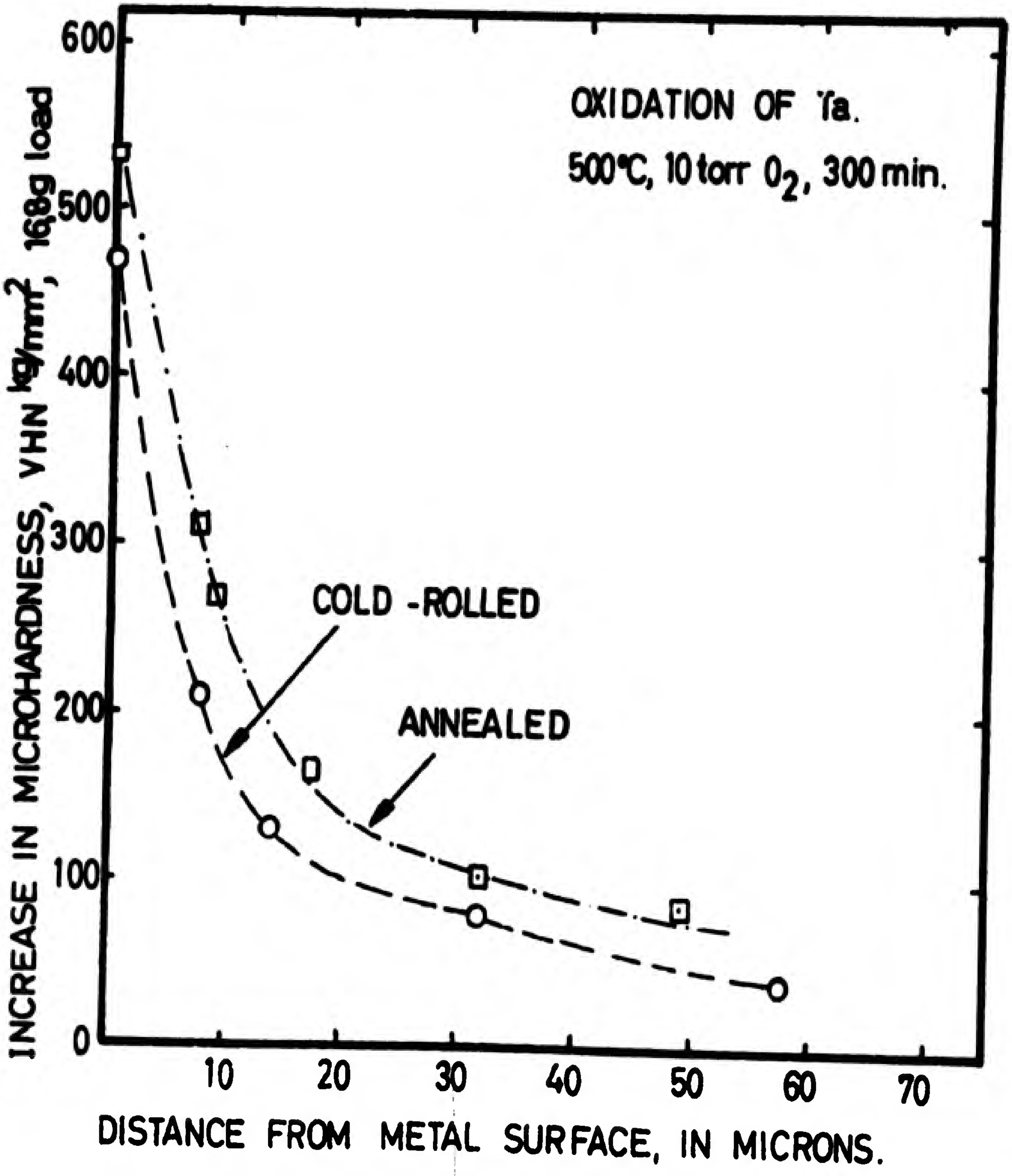

Fig. 22. Microindentation hardness as a function of distance from the metal surface. Cold-rolled and annealed Ta-specimens oxidized for 300 min. at 500 °C and 10 torr oxygen.

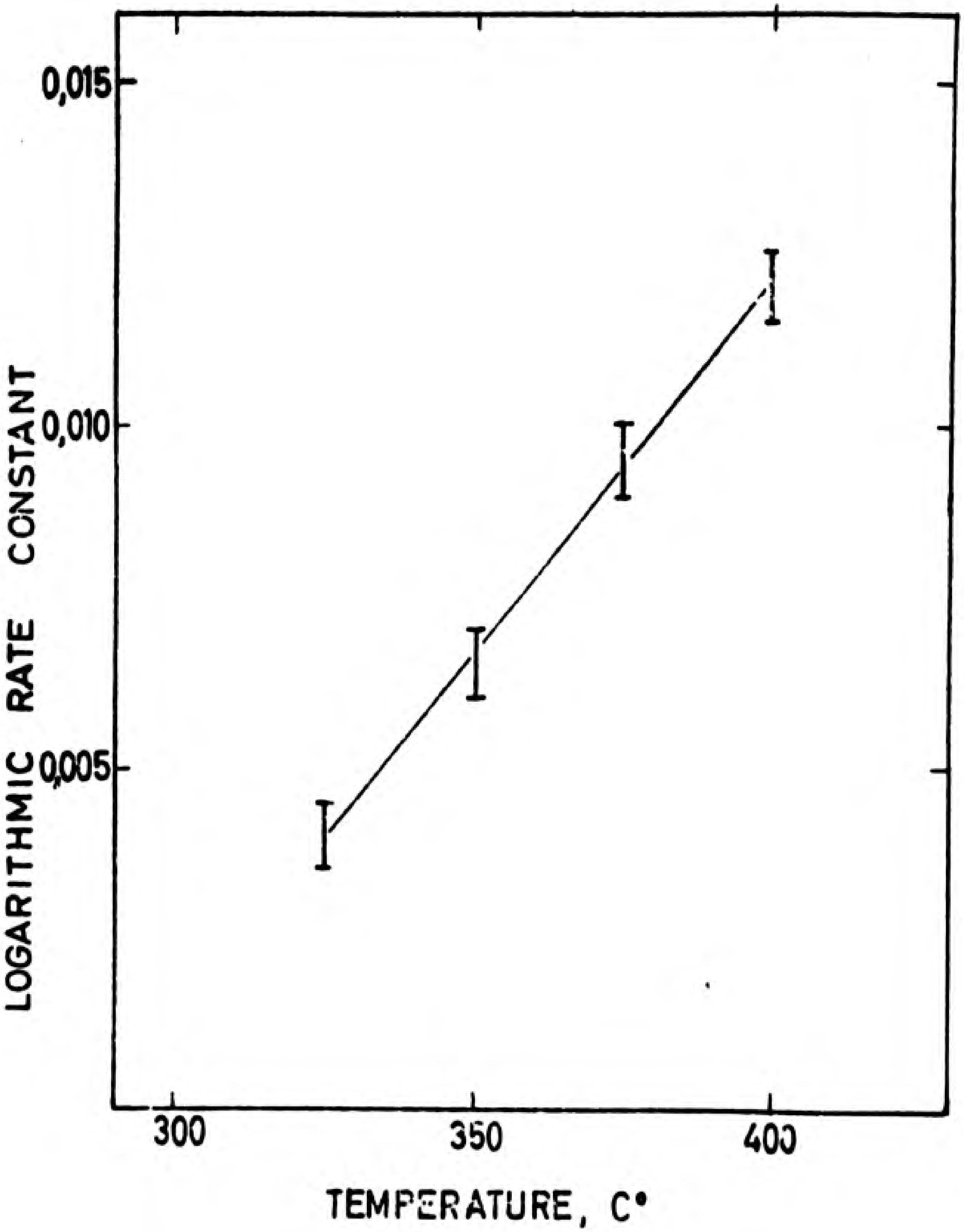

Fig. 23. The rate constant for the logarithmic oxidation of tantalum as a function absolute temperature.

Central Institute for Industrial
Research,
Blindern, Oslo, Norway
Rep. No. AD
Monitoring Agency:

Grant:
AF-EOAR-61-42
TN No. 3
Field: SSS

Oxidation of Tantalum in the Temperature Range 300° - $550\ ^\circ C$.

P. Kofstad

November 1961

ABSTRACT: Oxidation of tantalum at 300° to $550\ ^\circ C$ constitutes oxygen dissolution in the metal, formation of the metallic oxide phases TaO_y and TaO_z, and formation of Ta_2O_5. The oxidation conforms with a logarithmic oxidation during initial periods below $450\ ^\circ C$, and with parabolic oxidation over longer periods of time and during initial periods at higher temperatures. Above $450\ ^\circ C$ the initial parabolic oxidation is followed by a breakaway oxidation.

Office of Aerospace Research, Brussels, Belgium

Central Institute for Industrial
Research,
Blindern, Oslo, Norway
Rep. No. AD
Monitoring Agency:

Grant:
AF-EOAR-61-42
TN No. 3
Field: SSS

Oxidation of Tantalum in the Temperature Range 300° - $550\ ^\circ C$.

P. Kofstad

November 1961

ABSTRACT: Oxidation of tantalum at 300° to $550\ ^\circ C$ constitutes oxygen dissolution in the metal, formation of the metallic oxide phases TaO_y and TaO_z, and formation of Ta_2O_5. The oxidation conforms with a logarithmic oxidation during initial periods below $450\ ^\circ C$, and with parabolic oxidation over longer periods of time and during initial periods at higher temperatures. Above $450\ ^\circ C$ the initial parabolic oxidation is followed by a breakaway oxidation.

Office of Aerospace Research, Brussels, Belgium

Central Institute for Industrial
Research,
Blindern, Oslo, Norway
Rep. No. AD
Monitoring Agency:

Grant:
AF-EOAR-61-42
TN No. 3
Field: SSS

Oxidation of Tantalum in the Temperature Range 300° to $550\ ^\circ C$.

P. Kofstad

November 1961

ABSTRACT: Oxidation of tantalum at 300° to $550\ ^\circ C$ constitutes oxygen dissolution in the metal, formation of the metallic oxide phases TaO_y and TaO_z, and formation of Ta_2O_5. The oxidation conforms with a logarithmic oxidation during initial periods below $450\ ^\circ C$, and with parabolic oxidation over longer periods of time and during initial periods at higher temperatures. Above $450\ ^\circ C$ the initial parabolic oxidation is followed by a breakaway oxidation.

Office of Aerospace Research, Brussels, Belgium

Central Institute for Industrial
Research,
Blindern, Oslo, Norway
Rep. No. AD
Monitoring Agency:

Grant:
AF-EOAR-61-42
TN No. 3
Field: SSS

Oxidation of Tantalum in the Temperature Range 300° - $550\ ^\circ C$.

P. Kofstad

November 1961

ABSTRACT: Oxidation of tantalum at 300° to $550\ ^\circ C$ constitutes oxygen dissolution in the metal, formation of the metallic oxide phases TaO_y and TaO_z, and formation of Ta_2O_5. The oxidation conforms with a logarithmic oxidation during initial periods below $450\ ^\circ C$, and with parabolic oxidation over longer periods of time and during initial periods at higher temperatures. Above $450\ ^\circ C$ the initial parabolic oxidation is followed by a breakaway oxidation.

Office of Aerospace Research, Brussels, Belgium

The logarithmic and parabolic oxidation is associated with metallic oxide formation and oxygen dissolution in the metal and the breakaway oxidation with Ta_2O_5-formation.

The logarithmic and parabolic oxidation is associated with metallic oxide formation and oxygen dissolution in the metal and the breakaway oxidation with Ta_2O_5-formation.

The logarithmic and parabolic oxidation is associated with metallic oxide formation and oxygen dissolution in the metal and the breakaway oxidation with Ta_2O_5-formation.

The logarithmic and parabolic oxidation is associated with metallic oxide formation and oxygen dissolution in the metal and the breakaway oxidation with Ta_2O_5-formation.